INFLUENCE OF MOLECULAR INTERACTIONS ON ELASTIC PROPERTIES AND OXYGEN DIFFUSION IN POLYBUTYLENE TEREPHTHALATE POLYMER: A MOLECULAR DYNAMICS STUDY

A Thesis
Submitted to the Graduate Faculty
of the
North Dakota State University
of Agriculture and Applied Science

By

Muniyamuthu Raviprasad

In Partial Fulfillment
for the Degree of
MASTER OF SCIENCE

Major Department:
Civil Engineering

November 2012

Fargo, North Dakota

North Dakota State University
Graduate School

Title

Influence of Molecular Interactions on Elastic Properties and Oxygen Diffusion in PolyButylene Terephthalate Polymer: A Molecular Dynamics Study

By

Muniyamuthu Raviprasad

The Supervisory Committee certifies that this ***disquisition*** complies with North Dakota State University's regulations and meets the accepted standards for the degree of

MASTER OF SCIENCE

SUPERVISORY COMMITTEE:

Dr. Dinesh Katti
Co-Chair

Dr. Kalpana Katti
Co-Chair

Dr. Sivapalan Gajan

Dr. Dean C Webster

Approved:

11/09/2012	Dr. Eakalak Khan
Date	Department Chair

ABSTRACT

In most barrier applications, both mechanical and diffusion properties of the material are important. In this thesis the evaluation of molecular mechanisms responsible for the enhanced elastic properties of **P**olymer **C**lay **N**anocomposites (PCNs) and the molecular mechanisms of Oxygen diffusion in PolyButylene Terephthalate polymer are presented. Interaction energy between PCN constituents, conformational changes of polymer, interaction energy between Oxygen molecule and polymer, rate of Oxygen and Oxygen diffusion coefficient are evaluated. Molecular simulation studies of PolyButylene Terephthalate (PBT) clay nanocomposite and Nylon6 clay nanocomposite show that a higher crystallinity polymer such as PBT would require higher attractive and repulsive interactions with organic modifier in order to make significant change in the crystallinity of PBT in the nanocomposite and in turn enhance the elastic modulus and hardness. Molecular interactions energy between Oxygen molecule and polymer, change in polymer conformation caused by thermal energy assist the Oxygen molecule to diffuse through polymer.

ACKNOWLEDGEMENTS

This research was completed during my graduate study in the Department of Civil Engineering at North Dakota State University. This thesis would not have been achievable without the guidance of people who supported me throughout the time at NDSU.

I am grateful to Dr. Dinesh Katti and Dr. Kalpana Katti for their guidance and encouragement in this work. Both of my advisers contributed their knowledge and experience to guide me in the appropriate direction to achieve my graduate work.

I also thankful to the support of NSF-EPSCoR FlexEM grant for the work conducted. Further, I would like to acknowledge the computational resources provided by the NDSU Center for high performance computing.

TABLE OF CONTENTS

LIST OF TABLES

Table Page

LIST OF FIGURES

Figure Page

LIST OF ABBREVIATIONS

AMBER……..Assisted Model Building with Energy Refinement

CFF……Consistent Force Field

CHARMM…… Chemistry at HARvard Macromolecular Mechanics

MD……..Molecular Dynamics

Nylon6-PCN……. Nylon6 Clay Nanocomposites

NPT…….....Number, Particle and Temperature are constant

PBT…….....PolyButylene Terephthalate

PCN…….…… Polymer Clay Nanocomposites

PBT-PCN…….. Polybutylene Terephthalate Clay Nanocomposites

VDW……...Van Der Waals

LIST OF APPENDIX FIGURES

INTRODUCTION

Background

Polymer clay nanocomposites (PCNs) are widely researched material systems for a wide variety of applications in industry because of enhanced mechanical, thermal, optical and barrier properties. PCNs are categorized as intercalated and exfoliated PCNs and typically synthesized by adding a small amount of organically modified expansive nano sized clay. Therefore, PCN is composed of polymer, organic modifier and nano sized expansive clay. In exfoliated nanocomposites, nano sized clay is dispersed randomly within the polymer. The following schematic illustration shows the exfoliated nanocomposite.

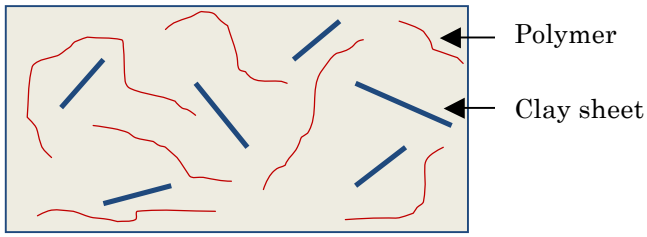

Figure 1.1. Schematic diagram of exfoliated clay in PCNs

In an intercalated nanocomposite, nano sized clay is dispersed randomly however layered clay structure is maintained. In this type nanocomposite, polymer chains fit in between clay sheets and clay sheets maintain the layered arrangement. The following schematic illustration shows the intercalated nanocomposites.

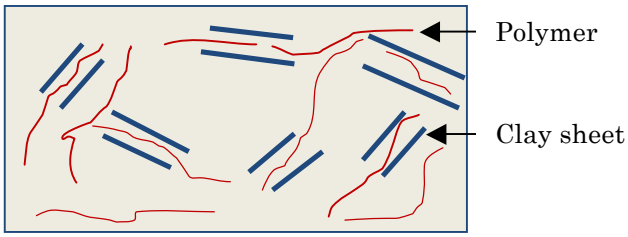

Figure 1.2. Schematic diagram of intercalated clay in PCNs

Polymer is the vital constituent in the PCN and it is a long chain sequentially composed of large number of monomers. Polymers can be characterized as natural polymer and synthesized polymer. Both of these polymers are hydrophobic in nature. Natural polymer includes protein, cellulose, etc. and synthetic polymer includes polyethylene, nylon, etc. The following schematic representation shows an example for the Polybutylene Terephthalate unit, which repeats in the polymer molecular model.

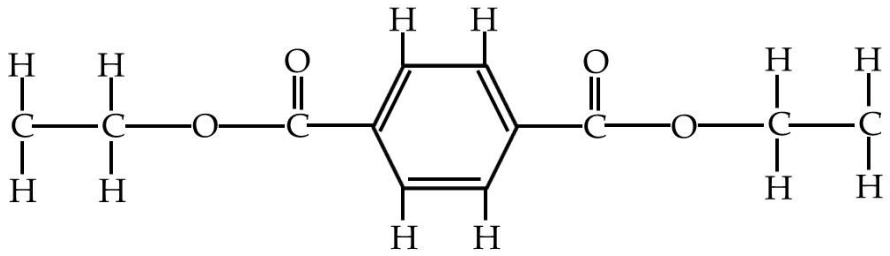

Figure 1.3. Schematic diagram of Polybutylene Terephthalate unit

Nano sized expansive clay is the important constituent in the PCNs. In general, expansive nano sized clay such as Na-Montmorillonite is used in the PCNs. Clay is a layered silicate structure and composed of two tetrahedral sheets and an octahedral sheet. The following schematic diagram shows the clay structure.

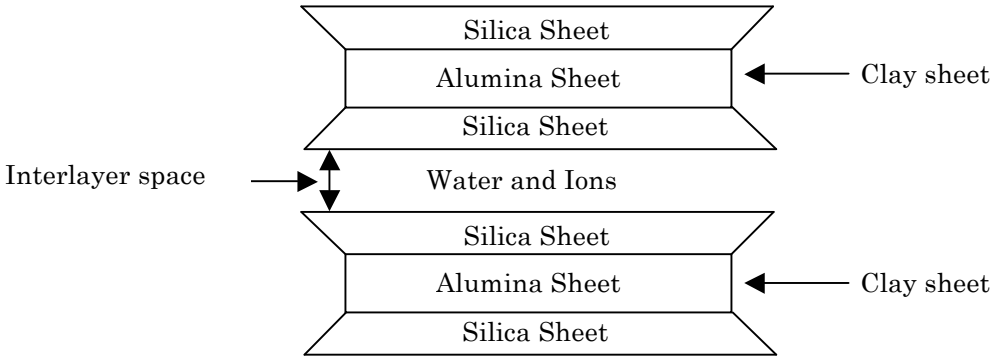

Figure 1.4. Schematic diagram of layered clay structure

Clay sheets have net negative charge, which is balanced by cations such as Sodium. The negative charge results because of isomorphous substitution and broken

edges in the clay sheet. Clay absorbs or loses water at the surface or interlayer spacing and therefore it is hydrophilic in nature. Modifying the clay using organic modifiers can alter the expansion and hydrophilicity of the clay.

Organic modifier is another important constituent in PCNs. Organic modifiers are used to modify the clay by replacing water and ions in the interlayer thus mix with hydrophobic polymer. This process allows polymer to enter into the interlayer of the clay sheets. Organic modifiers are sub-divided into functional groups and backbone chains. The following figure shows the schematic representation of a protonated 12-Aminolauric acid with functional groups and backbone chain.

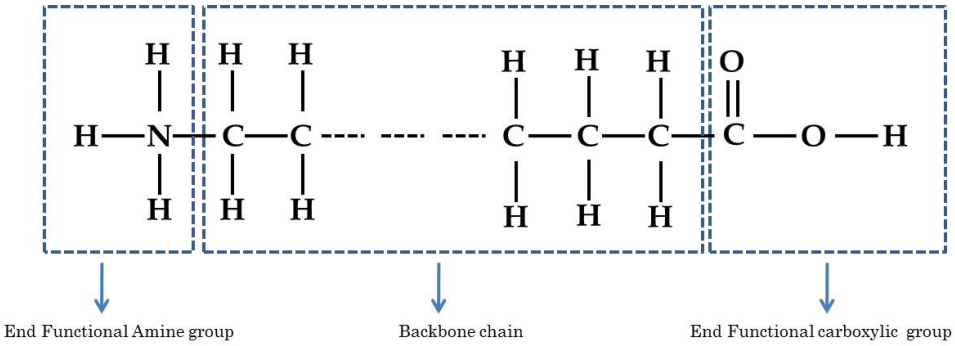

Figure 1.5. Schematic diagram of protonated 12-Aminolauric acid

Molecular dynamics (MD) is a computational method used to study the time dependent behavior of molecules and it is extensively used to study proteins, bio molecules, polymers, and minerals. MD provides detailed information of molecules in terms of interactions between molecules and conformational changes of molecules. This method involves solving the equation of motion in small time steps. The equation of motion:

$$\mathbf{F_i = m_i a_i}$$

Where F_i is the force acting on an atom i, m_i is the mass of an atom i and a_i is the acceleration of an atom i. This equation solves for a precise interatomic potentials with initial conditions and boundary conditions. Force acting on an atom is calculated from

the potential energy of the molecular system. The following equation describes the mathematical form for forces acting on atoms:

$$m_i \ddot{\vec{r}}_i = -\frac{\partial}{\partial \vec{r}_i} U_{total}(\vec{r}_1, \vec{r}_2, \ldots\ldots\ldots \vec{r}_N) \quad i = 1,2,3 \ldots\ldots N$$

U_{total} is the potential energy of the molecular system, $\ddot{\vec{r}}_i$ is the acceleration of an atom i. Change in potential energy of an atom i with respect to its position (r) is equal to the force acting on an atom i. By solving these equations, MD provides time dependent response for a molecular system. This response contains position of every atom in the system and their velocities over a time.

Potential energy of a molecular system can be described by using mathematical form called force field. Some of the general force fields used by researchers are CHARMM, CFF, and AMBER. Potential energy of any molecular system consists of bonded energy and non-bonded energy. Bonded energy includes bond stretching, angle bending and rotation about bond. The bond stretching energy is given by the following equation:

$$U_{bond} = \sum_{i=1}^{n} K_i^{bond} (r_i - r_{oi})^2$$

The definition for each term of the equation is presented in the appendix. This equation describes the energy when a covalent bond between two atoms stretches. The angle bending energy is given by the following:

$$U_{angle} = \sum_{i=1}^{n} K_i^{angle} (\theta_i - \theta_{oi})^2$$

The definition for each term of the equation is presented in the appendix. The above equation describes the energy when an angle between two pair of covalent bonds with a

shared atom at the vertex changes. The rotational energy can be derived in two different forms. The first form of such energies is given by the following equation:

$$\mathbf{U_{dihedral}} = \sum_{\mathbf{i=1}}^{\mathbf{n}} \mathbf{K_i^{dihedral}}[\mathbf{1} + \mathbf{cos}(\boldsymbol{n_i\varphi_i} - \boldsymbol{\varphi_{oi}})], \boldsymbol{n_i} \neq \mathbf{0}$$

The definition for each term of the equation is presented in the appendix. This equation describes the energy when three pair covalent bonds with a shared bond that subjected to torsional rotation. The second form of energy is given by the following equation:

$$\mathbf{U_{improper}} = \sum_{\mathbf{i=1}}^{\mathbf{n}} \mathbf{K_i^{improper}} (\mathbf{\emptyset_i} - \mathbf{\emptyset_{oi}})^2$$

The definition for each term of the equation is presented in the appendix. This equation describes the energy when a four planar, covalently two double-bond and a covalent bond atoms changes the angle between them. The bonded energy terms are depicted in the following figure.

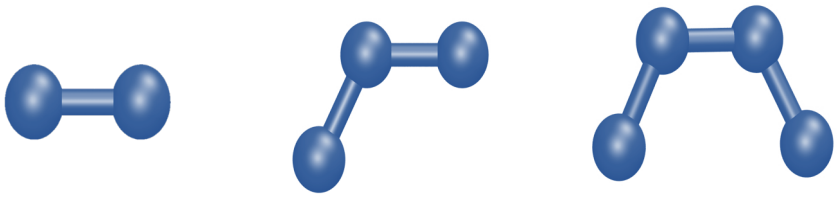

Figure 1.6. Schematic representation of bond, angle and dihedral stretching

The non- bonded energy consists of van der Waals energy and electrostatic energy of the molecular system. The following equation represents the van der Waals interaction:

$$\mathbf{U_{vdW}} = \sum_{\mathbf{i}} \sum_{\mathbf{j>1}} \mathbf{4}\varepsilon_{\mathbf{ij}} \left[\left(\frac{\sigma_{\mathbf{ij}}}{\mathbf{r_{ij}}} \right)^{\mathbf{12}} - \left(\frac{\sigma_{\mathbf{ij}}}{\mathbf{r_{ij}}} \right)^{\mathbf{6}} \right]$$

The following equation represents the electrostatic interaction:

$$\mathbf{U_{coulomb}} = \sum_{\mathbf{i}} \sum_{\mathbf{j>1}} \frac{\mathbf{q_i q_j}}{\mathbf{4}\pi\varepsilon_{\mathbf{o}}\mathbf{r_{ij}}}$$

The definition for each term of the equation is presented in the appendix.

Finally, total potential energy of the molecular system can be described as a sum of all the individual functions as follows:

$$\mathbf{U}_{total} = \mathbf{U}_{bond} + \mathbf{U}_{angle} + \mathbf{U}_{dihedral} + \mathbf{U}_{improper} + \mathbf{U}_{vdW} + \mathbf{U}_{coulomb}$$

These individual potential energy terms can be described by mathematical functions as shown above and those functions depend on spring constants, initial conditions and variables.

Problem Description

In most barrier applications, both mechanical and diffusion properties of the material are important. The objective of this master thesis was to understand the fundamental mechanisms responsible for the enhanced elastic modulus and hardness of Polybutylene Terephthalate Clay Nanocomposite and the molecular mechanisms of Oxygen gas diffusion in Polybutylene Terephthalate polymer. A molecular simulation approach was used to uncover the mechanisms at the atomistic scale. The goal was to evaluate the molecular interaction between Polybutylene Terephthalate clay nanocomposites constituents and the interaction between Oxygen molecule and Polybutylene Terephthalate polymer, conformational changes in Polybutylene Terephthalate polymer.

Disposition

This thesis composed of five chapters and an appendix. First chapter describes the general information about polymer clay nano composites, objectives of this work and organization of this thesis. The second chapter describes the works done previously related to polymer clay nanocomposites. Then, third and fourth chapters explain the work completed on Polybutylene terephthalate clay nanocomposites and diffusion of Oxygen gas in Polybutylene terephthalate polymer respectively. Final chapter describes the work that can be done in the future.

LITERATURE REVIEW

Review

Polymer Clay Nanocomposites (PCNs) are used in various applications such as automobile, aviation, biomedical and polymer related applications. Toyota R&D labs developed the first PCN in 1985 in Japan and they pioneered in clay nanocomposites for twenty-five years[1]. Since 1985, many researchers developed PCNs with different polymers such as Nylon6, Polyethylene, and Polyolefin[2]. PCN composed of Nylon6 was studied extensively[2-5]. Polymer clay nanocomposites are categorized as intercalated and exfoliated PCNs and are typically synthesized by adding about 1-9 % of weight of polymer of organically modified expansive nano sized clay[3,6]. Among three constituents in PCNs, polymer is the major in quantity. PCNs can be synthesized using solution intercalation, in-situ polymerization and melt blending. Addition of organically modified clay enhances the mechanical properties[7], thermal properties[8-10] and barrier properties[8,10-13] of polymer clay nanocomposites. Most importantly, the amount of clay in PCN influences the crystallinity of polymer and the mechanical properties[14]. Studies show that the properties of PCNs depend on individual phases and interaction between individual constituents [2,4,14]. Previous works on PCNs have shown that the non- bonded interactions between different constituents alter polymer phase [2,4,14] and thus significantly influence the mechanical properties of PCNs[3]. The organic modifier which is used to modify the clay, has a significant influence on crystallinity of polymer and elastic modulus of PCNs[2]. Effect of different organic modifiers, which contains different functional groups and different chain lengths, are studied with Nylon6 in detail [2]. Any detail information of Nylon6-PCN can be found readily in online journals or articles. The results indicate that the functional group and backbone chain length of organic modifier

have a significant influence on d- spacing of PCNs, crystallinity of polymer and the elastic modulus of PCNs.

In this work, I focused on developing Polybutylene terephthalate clay nanocomposites for the application of flexible electronics coatings. Polybutylene terephthalate (PBT) is a semi-crystalline thermoplastic polymer which shows excellent properties such as rate of crystallization and thermal stability [15]. PBT has been used widely in nanocomposites [16-19] and show improved tensile modulus and strength[19], enhanced thermo mechanical properties and elastic modulus[10]. High viscosity PBT nanocomposites show improved mechanical, dynamic mechanical properties [18]. Several experimental studies conducted on PBT clay nanocomposites can be found in the literature [10,15-25]. Mechanical properties of Nylon6-PCN are studied at molecular scale using molecular dynamics and experiments [2,4,5,14,26-28]. In this work, I studied molecular mechanism responsible for enhanced elastic modulus and hardness of Polybutylene terephthalate clay nanocomposites using molecular dynamics simulation.

Diffusion of Oxygen gas in polymers is an important property in many areas related to polymer engineering. In practice, it controls quality of coatings, separation process of membrane, food packing and bio medical devices[29]. Therefore, understanding the mechanism of diffusion in polymeric systems enables us to improve the barrier properties of polymers and polymer related nanocomposites such as polymer clay nanocomposites. Many researchers conducted molecular dynamics study to understand the mechanism of diffusion of small molecules, such as O_2, N_2 and CO_2, in polymeric system[29-42]. Particularly, researchers studied diffusion of Oxygen gas in different polymers, such as PET[29], Polystyrene[38], using molecular dynamics simulation. Pavel and Shanks investigated diffusion coefficient of O_2 and CO_2 in Polyethylene terephthalate polymer at different temperatures[29,31,41]. They studied influence of temperature, polymer dynamics, and number of aromatic rings, density and free volume on diffusion

coefficient. Takeuchi studied self-diffusion coefficient of O_2 and relaxation times of internal rotations of the Polymethylene chains at different temperatures[30]. He also found that the free volume influences O_2 diffusion. Muller-Plathe investigated diffusion coefficient of H_2, O_2 and CH_4 in Polypropylene[36,39]. However, detailed study of diffusion mechanism in terms of interactions and conformations of polymer has not been reported. In this work, I investigated the Oxygen diffusion in Polybutylene terephthalate polymer. Diffusion in semi crystalline polymers is very slow[36] therefore PBT polymer is a good candidate to investigate the diffusion mechanism. I investigated O_2 diffusion, interaction energy between O_2 and polymers and influence of conformational changes of polymers.

References

1. Okada, A.; Usuki, A. Macromolecular Materials and Engineering **2006,** 291, (12), 1449-1476.
2. Sikdar, D.; Katti, D. R.; Katti, K. S.; Mohanty, B. International Journal of Nanotechnology **2009,** 6, (5-6), 468-492.
3. Sikdar, D.; Pradhan, S. M.; Katti, D. R.; Katti, K. S.; Mohanty, B. Langmuir **2008,** 24, (10), 5599-5607.
4. Sikdar, D.; Katti, K. S.; Katti, D. R. Journal of Nanoscience and Nanotechnology **2008,** 8, (4), 1638-1657.
5. Sikdar, D.; Katti, D. R.; Katti, K. S. Journal of Applied Polymer Science **2008,** 107, (5), 3137-3148.
6. Bandyopadhyay, J.; Sinha Ray, S. Polymer **2010,** 51, (6), 1437-1449.
7. Giannelis, E. P. Advanced Materials **1996,** 8, (1), 29-&.
8. Barick, A. K.; Tripathy, D. K. Polymer Engineering and Science **2010,** 50, (3), 484-498.
9. Wang, Y. M.; Gao, J. P.; Ma, Y. Q.; Agarwal, U. S. Composites Part B-Engineering **2006,** 37, (6), 399-407.
10. Chow, W. S. Journal of Applied Polymer Science **2008,** 110, (3), 1642-1648.
11. Herrera Alonso, R.; Estevez, L.; Lian, H.; Kelarakis, A.; Giannelis, E. P. Polymer **2009,** 50, (11), 2402-2410.
12. Burgaz, E.; Lian, H.; Alonso, R. H.; Estevez, L.; Kelarakis, A.; Giannelis, E. P. Polymer **2009,** 50, (11), 2384-2392.
13. Lao, S. C.; Wu, C.; Moon, T. J.; Koo, J. H.; Morgan, A.; Pilato, L.; Wissler, G. J ournal of Composite Materials **2009,** 43, (17), 1803-1818.
14. Sikdar, D.; Katti, D.; Katti, K.; Mohanty, B. Journal of Applied Polymer Science **2007,** 105, (2), 790-802.

15. Xiao, J. F.; Hu, Y.; Wang, Z. H.; Tang, Y.; Chen, Z. Y.; Fan, W. C. European Polymer Journal **2005,** 41, (5), 1030-1035.
16. Chang, J.-H.; An, Y. U.; Kim, S. J.; Im, S. Polymer **2003,** 44, (19), 5655-5661.
17. Wu, F.; Yang, G. Materials Letters **2009,** 63, (20), 1686-1688.
18. Chang, Y. W.; Kim, S.; Kyung, Y. Polymer International **2005,** 54, (2), 348-353.
19. Shyang, C. W., Tensile and Thermal properties of Poly(Butylene Terephtalate)/Organo-Montmorillonite Nanocomposites. Malaysian polymer Journal: 2008; Vol. 3, pp 1-13.
20. Hong, Y.; Yoon, H. G.; Lim, S. International Journal of Precision Engineering and Manufacturing **2009,** 10, (3), 115-118.
21. Mu, B.; Wang, Q. H.; Wang, T. M.; Wang, H. G.; Jian, L. Q.; Pei, X. Q. Polymer Composites **2009,** 30, (5), 619-628.
22. Nirukhe, A. B.; Shertukde, V. V. Journal of Applied Polymer Science **2009,** 113, (1), 585-592.
23. Acierno, D.; Scarfato, P.; Amendola, E.; Nocerino, G.; Costa, G. Polymer Engineering and Science **2004,** 44, (6), 1012-1018.
24. Wan, C. Y.; Bao, X. J.; Zhao, F.; Kandasubramanian, B.; Duggan, M. P. Journal of Applied Polymer Science **2008,** 110, (1), 550-557.
25. Wu, D. F.; Zhou, C. X.; Yu, W.; Fan, X. Journal of Polymer Science Part B-Polymer Physics **2005,** 43, (19), 2807-2818.
26. Sikdar, D.; Katti, D. R.; Katti, K. S. Langmuir **2006,** 22, (18), 7738-7747.
27. Katti, K. S.; Sikdar, D.; Katti, D. R.; Ghosh, P.; Verma, D. Polymer **2006,** 47, (1), 403-414.
28. Sikdar, D.; Katti, D. R.; Katti, K. S.; Bhowmik, R. Polymer **2006,** 47, (14), 5196-5205.
29. Pavel, D.; Shanks, R. Polymer **2005,** 46, (16), 6135-6147.
30. Takeuchi, H.; Okazaki, K. Journal of Chemical Physics **1990,** 92, (9), 5643-5652.
31. Pavel, D.; Shanks, R. Polymer **2003,** 44, (21), 6713-6724.
32. Neyertz, S.; Brown, D. Macromolecules **2009,** 42, (21), 8521-8533.
33. Neyertz, S.; Brown, D. Macromolecules **2008,** 41, (7), 2711-2721.
34. Karlsson, G. E.; Gedde, U. W.; Hedenqvist, M. S. Polymer **2004,** 45, (11), 3893-3900.
35. Liu, Q. L.; Huang, Y. Journal of Physical Chemistry B **2006,** 110, (35), 17375-17382.
36. Mullerplathe, F. Journal of Chemical Physics **1992,** 96, (4), 3200-3205.
37. Kucukpinar, E.; Doruker, P. Polymer **2003,** 44, (12), 3607-3620.
38. Mozaffari, F.; Eslami, H.; Moghadasi, J. Polymer **2010,** 51, (1), 300-307.
39. Mullerplathe, F. Journal of Chemical Physics **1995,** 103, (10), 4346-4351.
40. Neyertz, S.; Brown, D.; Pandiyan, S.; van der Vegt, N. F. A. Macromolecules **2010,** 43, (18), 7813-7827.
41. Shanks, R.; Pavel, D. Molecular Simulation **2002,** 28, (10-11), 939-969.
42. Wu, S. Z.; Yi, J.; Zhang, L. S.; Zhang, L. Q.; Mark, J. E. International Journal of Modern Physics B **2008,** 22, (31-32), 5859-5864.

POLY BUTYLENE TEREPHTHALATE CLAY NANOCOMPOSITES

Introduction

Molecular dynamics simulation was used to investigate the mechanisms responsible for the enhanced elastic modulus and hardness of Polybutylene Terephthalate Clay Nanocomposite. Polybutylene Terephthalate Clay Nanocomposite was considered for the application of coatings in flexible electronics products. The primary approach was to quantify the interaction energies between Polybutylene terephthalate clay nanocomposites constituents thus understanding the crystallinity change of PBT polymer in its clay nanocomposites.

In this work, the PCN containing PBT is referred to as PBT-PCN and PCN containing Nylon6 is referred to as Nylon6-PCN. These two material systems consist of same amount of nano sized clay and same number of organic modifiers. Interaction energies were calculated between polymer and clay, polymer and organic modifier, organic modifier and clay. The change in polymer conformation was investigated. Following sections explain molecular model construction, simulations, polymer conformations, and interactions energy between PBT-PCN constituents in detail. The comparison of PBT-PCN interaction energy with Nylon6-PCN interactions was done in order to understand the molecular mechanisms responsible for the enhanced elastic modulus and hardness of PCNs.

Computational Methods

Molecular dynamics simulation was used to study the interactions between atoms and group of atoms in PBT-PCN and Nylon6-PCN. Molecular dynamics simulations provide an insight into mechanisms responsible for the enhancement of PCN properties. NAMD[1] and VMD [2] were used to perform Molecular Dynamics (MD) simulations and post processing analyses respectively. NAMD Energy module was used

to calculate interaction energy between organically modified clay constituents and PCN constituents. Materials Studio was used to construct molecular models and generate initial coordinates. The molecular structure information was obtained using TopoTools plug-in that is available in VMD. CHARMM force field parameters were used for Nylon6, 12-Aminolauric acid and clay. Force field parameters for PBT were obtained by considering number of methyl group and model components which are similar to Polyethylene Terephthalate[3]. All the simulations were performed using 12 numbers of parallel processors. Each processor has 2.66 Ghz speed and one terabyte of distributed memory.

PBT monomers are used to build polymers. Six different lengths of PBT polymer models were built to study the length effect of polymers on d-spacing of clay in PCNs. These models contain two, four, six, eight, ten and twelve units. All PBT polymer models were annealed at 700 K under atmospheric pressure. Annealing process was conducted three times to obtain globally minimized confirmation of PBT chains and minimization was confirmed from the potential energy. The following table summarizes the PBT models.

Table 3.1. PBT polymer model descriptions

Model	Number of units	Molecular mass (amu)
1	2	386.4
2	4	772.8
3	6	1159.2
4	8	1545.6
5	10	1932.0
6	12	2318.4

The clay was modified using 12-Aminolauric acid in order to increase the interlayer spacing between clay sheets. This increment allows polymer to stay in between clay sheets. The intercalated polymer clay nanocomposite system was mimicked through molecular simulations. Partial charges of a unit of protonated 12-aminolauric acid are shown in figure 3.1.

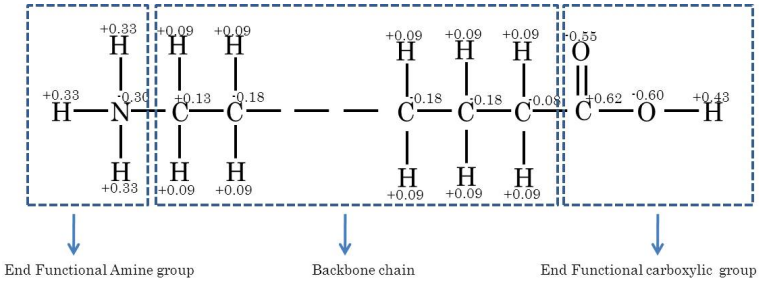

Figure 3.1. Scehamatic diagram of protonated 12-Aminolauric acid with partial charges

Na-Montmorillonite (Na-MMT) was used as a nano sized clay particle. Two clay sheets were used to build molecular model. Each sheet consists of eighteen unit cells where six unit cells are in X direction and three unit cells are in Y direction. The following figure shows the molecular clay model.

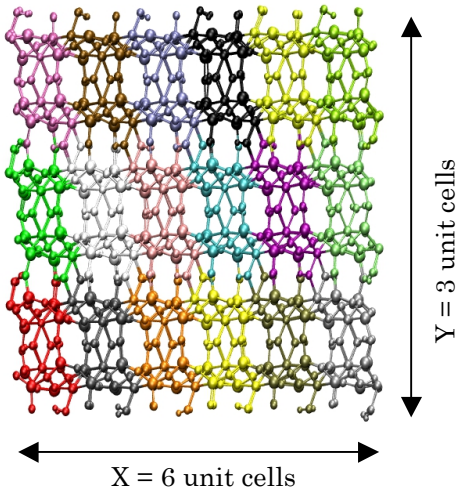

Figure 3.2. Planar view of the molecular clay model

Organically Modified Montmorillonite (OMMT) model consists of two sheets of montmorillonite (MMT) and eighteen numbers of 12-aminolauric acid molecules. Size of the OMMT model is 31.68 Å in X direction, 27.44 Å in Y direction and 24.16 Å in Z direction. Each of MMT sheets has nine sodium cations and these sodium ions are replaced by 9 number of 12-Aminolauric acid. Each of these 12-Aminolaueic acids has a net positive charge equivalent to sodium ion. In order to make OMMT model charge

neutral, eighteen numbers of 12-Aminolauric acid molecules are inserted in the model where nine are inserted in between two MMT sheets and nine are inserted above the MMT sheet as shown in the figure 3.3. 12-Aminolauric acid molecules are placed flat and parallel to the MMT sheet. Five different organically modified clay (OMMT) models were built to identify the appropriate initial OMMT model. These five initial d-spacing are shown in the table 3.2.

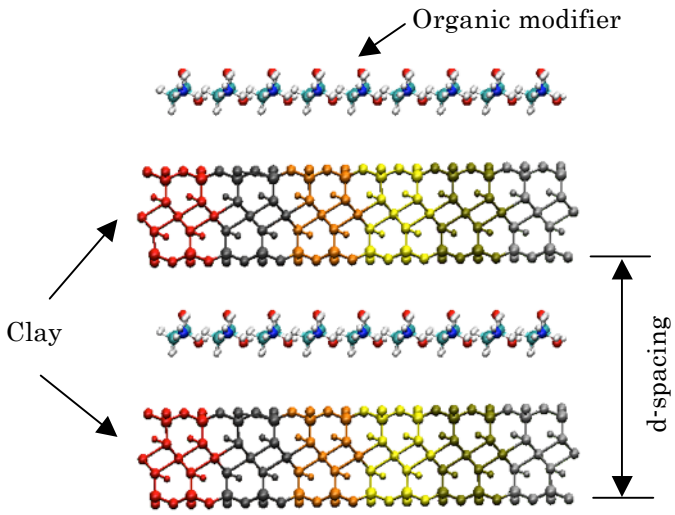

Figure 3.3. Molecular model of an initial OMMT

Table 3.2. Initial d-spacing of different OMMT models

Model	Initial d-spacing (Å)
1	15.60
2	16.60
3	17.60
4	18.60
5	19.60

First, OMMT model was minimized for 25 ps at temperature of zero Kelvin in vacuum using molecular dynamics program NAMD. Next, the temperature of the OMMT system is raised to 300 K in three equal steps by Langevin temperature parameter. Once the temperature is increased to 300 K, pressure of the OMMT system is increased to 1.01325 bars in four equal steps by Langevin piston pressure control.

Then, the system temperature is increased by 33 K and subsequently reduced to atmospheric temperature. The increase and reduction of temperature is done to mimic the experimental conditions[4]. A 0.5 fs time step is used for all OMMT simulations. Finally, OMMT model is simulated for 100 ps at room temperature and pressure with periodic boundary condition. During OMMT simulation, constraints were applied to MMT atoms in X and Y direction but MMT atoms are allowed to move in Z direction. There are no constraints applied to organic modifiers thus organic modifier atoms are allowed to move in all three directions. Simulation of OMMT is done under constant number of particles, constant pressure and constant temperature (NPT). 16Å cut off distance and 14Å switch distance are used for van der Waals and electrostatic energy calculation in all simulations.

Selected OMMT model and minimized PBT models are used to construct PCN models. Six different lengths of PBT chains are used in PCN to select the suitable PCN system. The suitable OMMT system is selected based on the d-spacing obtained from MD simulation and XRD experiment. The detail explanation is given in the results section below. One of the initial PBT-PCN models is shown in figure 3.4 and the estimated mass of PBT chains in PCN model with respect to clay is shown in table 3.3.

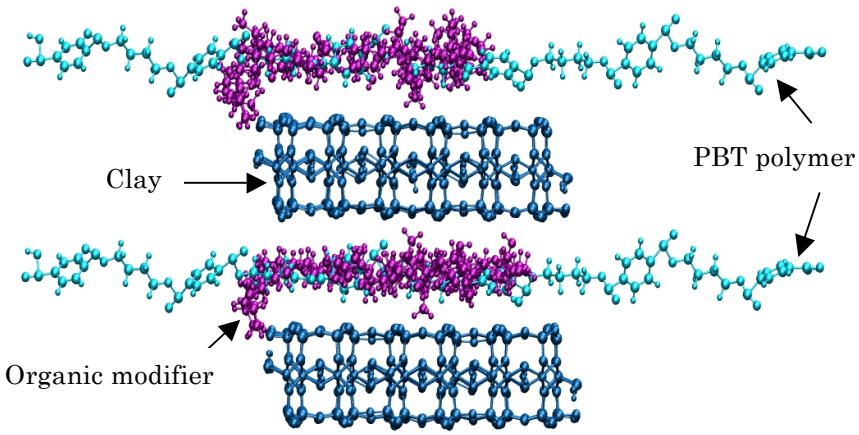

Figure 3.4. Initial molecular model of PBT-PCN

Table 3.3. Mass description of PCN models

Model	Intercalated polymer wt % with clay
PCN(1)	1.96
PCN(2)	4.19
PCN(3)	6.41
PCN(4)	8.64
PCN(5)	10.87
PCN(6)	13.10

Two PBT chains are inserted into the OMMT model and one is placed in between clay sheets and the other is placed above the top clay sheet to ensure the periodic boundary condition during the simulation. Physical dimensions of PBT are measured and compared with the simulated interlayer spacing of OMMT to make sure that the PBT chain fits in the model. The same conditions described above were implemented to construct the nylon6-PCN model. The number of Nylon6 chains in PCN model is selected based on the previous work[5]. Initial Nylon6-PCN model is shown in the figure 3.5.

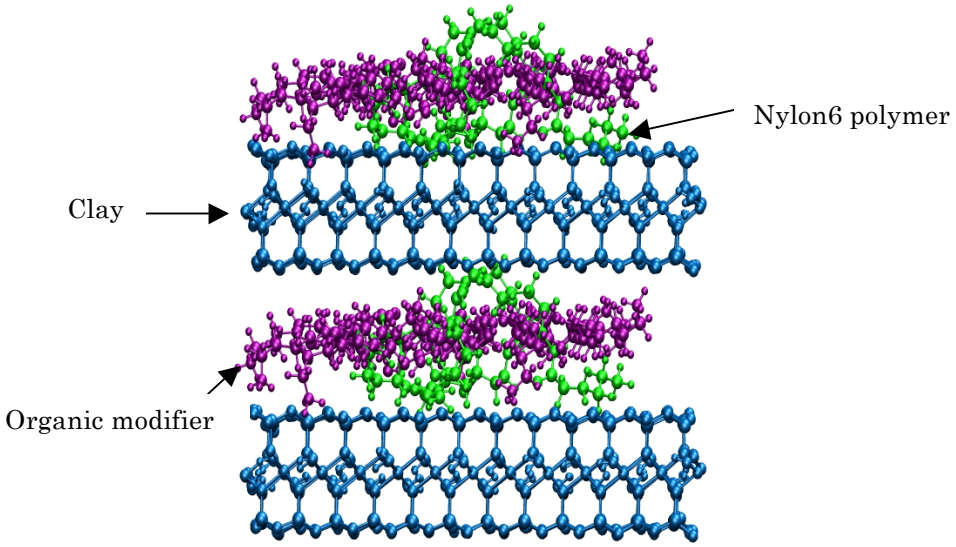

Figure 3.5. Initial molecular model of Nylon6-PCN

Molecular simulation is conducted for PBT-PCN and Nylon6-PCN systems. Procedure for minimization and dynamics of PCNs is performed as described in OMMT

simulation. Cell basis vector for PCNs is adjusted according to the physical size of different models. Periodic boundary conditions are applied to calculate the electrostatic interactions between PCN constituents. Initially, PCN models are simulated for 25 ps. Based on the d-spacing, final PCN model is selected and then the final simulation is conducted for 200 ps. Constraints are applied to MMT as mentioned in OMMT simulation and polymers are allowed to move freely in all three directions. Constant number, pressure and temperature (NPT) are used for all PCN simulation. Constant pressure is maintained by Nose'-Hoover Langevin piston pressure control method. This method is used with Langevin dynamics, such as temperature control, in order to perform NPT ensemble. Equilibrium of PCN system is confirmed from the plot of total energy of the system vs. simulation time. It was found that 200 ps simulation time is sufficient for the PCN simulations. Final model is selected based on the experimental d-spacing.

Results and Discussion

First, d-spacing was measured from the results obtained from OMMT simulations and compared with experimental d-spacing[4]. Experimental d-spacing was measured for several samples and the range varies between 15.60 Å to 17.43 Å. Among five different initial d-spacing of OMMT models, d-spacing of 17.60 Å OMMT model predicts final d-spacing of 15.50 Å which is very close to experimental d-spacing of 15.60 Å. OMMT model is chosen for PCN simulation based on the d-spacing comparison. The table 3.4 shows the d-spacing comparison between simulated values and experimental value for all five models.

Table 3.4. OMMT d-spacing comparison

Model	Initial d-spacing (Å)	Final d-spacing (Å)	Experimental d-spacing (Å)[4]
1	15.60	14.10	
2	16.60	14.95	
3	17.60	15.50	15.60
4	18.60	14.65	
5	19.60	14.93	

The non-bonded interaction, van der Waals energies and electrostatic energy, between different constituents in OMMT were calculated. Two different groups of atoms in the organic modifier were identified, which are functional group atoms, and backbone atoms. Therefore, non-bonded interaction energies between functional group atoms and clay, and backbone atoms and clay were calculated. Results show that electrostatic interaction dominates among the non-bonded interaction. The following table summarizes the interaction energies between clay and atom groups in the organic modifier.

Table 3.5. Interaction energy between clay and modifier components

Component of modifier and clay	Electrostatic energy (kcal/mole) [Col-A]	van der Waals energy (kcal/mole) [Col-B]	Total non-bonded energy (kcal/mole) [Col-A + Col-B]
Clay-Modifier backbone hydrogen	-2503	-87	-2590
Clay-Modifier backbone carbon	+1954	-257	+1697
Clay-Modifier functional hydrogen	-2392	-8	-2400
Clay-Modifier functional nitrogen	+497	-0.5	+497
Clay-Modifier functional oxygen	+1689	-48	+1641
Clay-Modifier functional carbon	-890	-25	-915

Interaction energy results show that organic modifier functional group interact more with clay electrostatically. Although individual atoms show repulsive interaction with clay, overall it shows attractive interaction with clay. Positive values indicate repulsive interactions and negative values indicate attractive interactions and higher magnitude denotes greater interactions. Interaction energy values of organic modifiers are the sum of backbone and functional group interaction energies. Between these two components, functional group of organic modifier shows higher interaction with clay than the backbone of the organic modifier. This is because of higher positive net charge in the functional group compared to the backbone. The table 3.6 shows the overall interaction energies between clay and organic modifier. Functional group interactions are composed of -1096 kcal/mol in electrostatic interaction energy and -80 kcal/mol in van der Waals interaction energy and backbone interactions are composed of -549

kcal/mol in electrostatic interaction energy and -345 kcal/mol in van der Waals interaction energy. Based on the values shown in the table 3.6, the electrostatic interactions are the major components in both modifier functional group and modifier backbone group.

Table 3.6. Overall interaction energies between clay and organic modifier groups

Component of modifier and clay	Electrostatic energy (kcal/mole)	van der Waals energy (kcal/mole)
Clay-Modifier backbone	-549	-345
Clay-Modifier functional group	-1096	-80

Based on the results shown in the table 3.5, the major component of attractive interactions results from the hydrogen atoms. Even though the partial charge of the backbone hydrogen smaller compared to functional group hydrogen as shown in figure 3.1, backbone hydrogen shows higher interaction because of its presence in significant numbers. The following table shows the total non-bonded interaction between clay and modifier groups.

Table 3.7. Total non-bonded interaction between clay and organic modifier

OMMT constituents	Non-bonded energy (kcal/mole)
Clay-Modifier backbone	-894
Clay-Modifier functional group	-1176

It is observed from the figure 3.6, the organic modifier spread entire surface area of the clay. Most importantly, amine functional groups in the organic modifier pointing towards the clay surface which validates the greater interaction in functional groups than in backbone with clay.

Six different polymer models for the model preparation of PCN were constructed. First, the polymer models were minimized and then physical dimension of the polymer models were measured. This measurement was performed in order to place the polymer chains in between clay sheets without any interference with clay atoms. Once the

dimensions were measured, polymer chains were inserted in between clay sheets. The figure 3.7 shows the conformation of polymer models after the minimization. Model-1 has physical dimension that is greater than the interlayer spacing of clay sheets. Therefore, model-1 was not used to construct the PCN models.

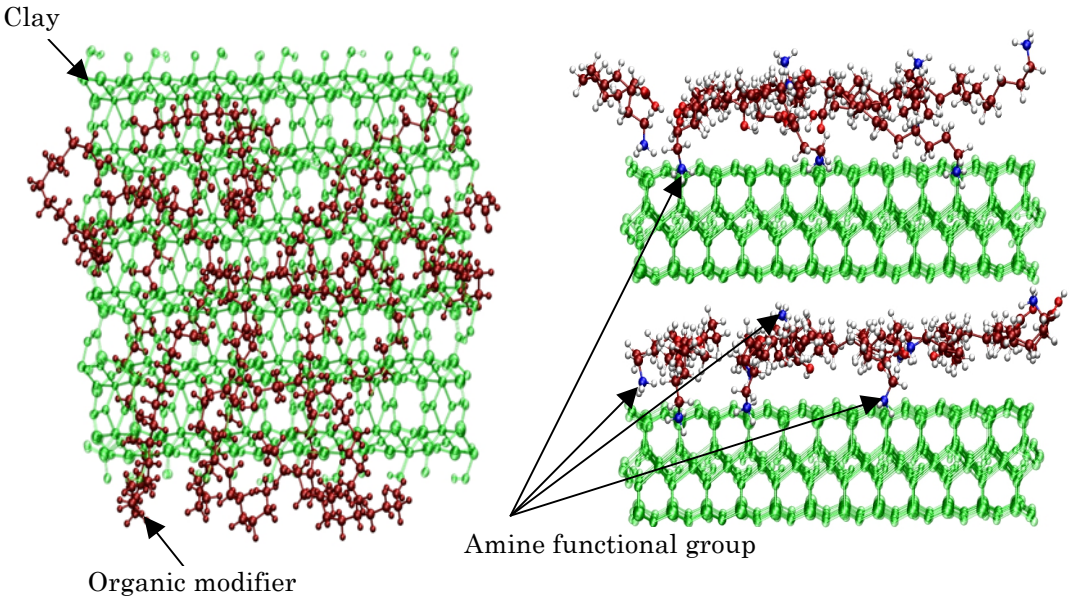

Figure 3.6. Orientation of organic modifier in the clay sheets

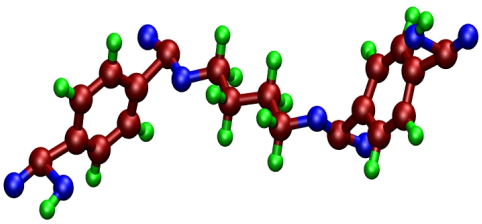

(a). Model-1

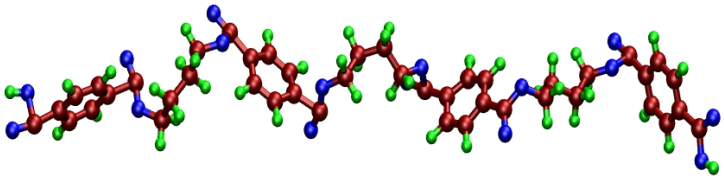

(b). Model-2

Figure 3.7. Conformations of individual polymer model

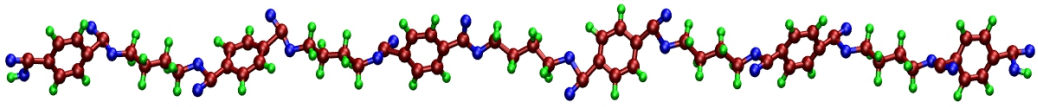

(c). Model-3

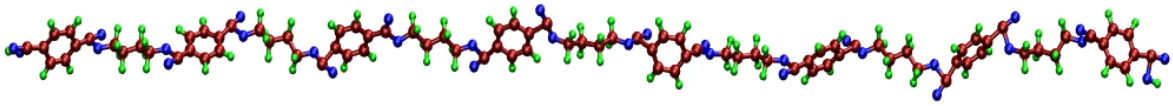

(d). Model-4

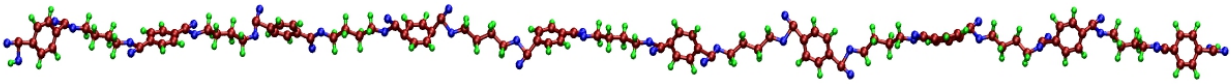

(e). Model-5

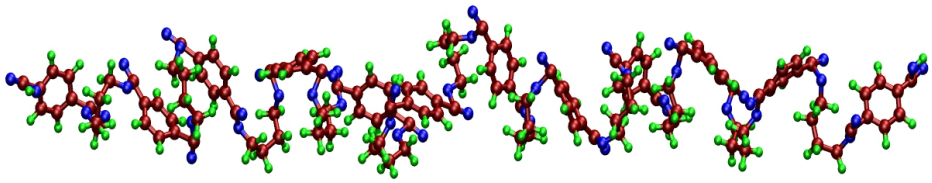

(f). Model-6

Figure 3.7. Conformations of individual polymer model (continued)

The d-spacing of all five PCN models was measured. Among five different PCN models, the PCN model which contains 6.41 wt% of PBT shows the simulated d-spacing

of 14.80 Å which is close to the experimental d-spacing of 14.53 Å. The same OMMT model with Nylon6 is simulated and it shows d-spacing of 15.35 Å. The following table summarizes the simulated d-spacing and experimental d-spacing of PCNs models

Table 3.8. PCNs d-spacing comparison

Model	Initial d-spacing (Å)	Final d-spacing (Å)	Experimental d-spacing (Å)[4]
PCN(2)		15.10	
PCN(3)		14.80	
PCN(4)	15.50	15.40	14.53
PCN(5)		15.00	
PCN(6)		16.00	

The conformation of polymer in the final stage for the model PCN (3) was observed. This model shows the d-spacing which is very close to the experimental value. The following figures show the conformation of PCN (3) model and Nylon6 PCN model.

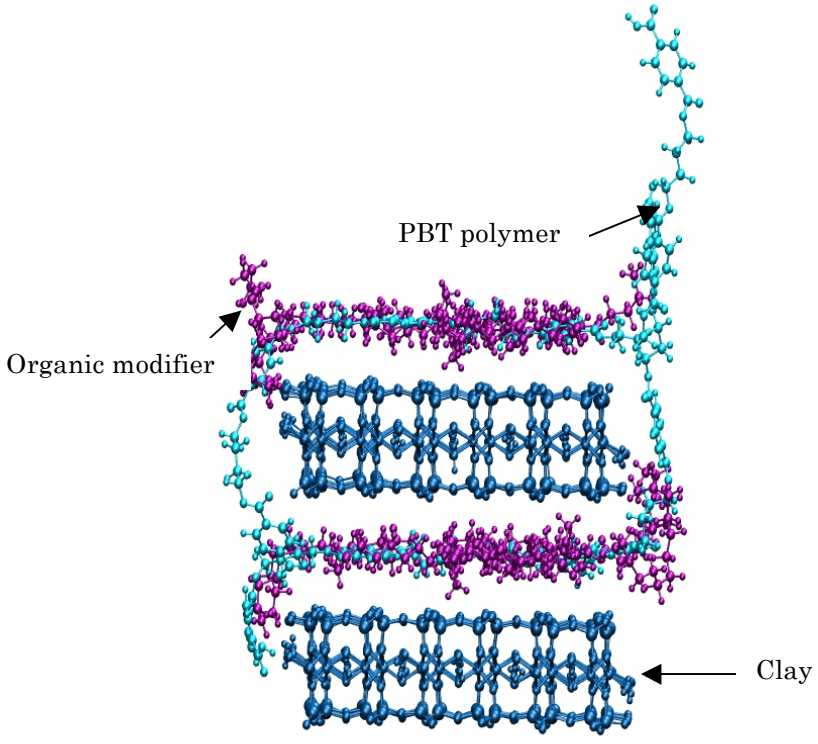

Figure 3.8. Final molecular conformation of PBT-PCN

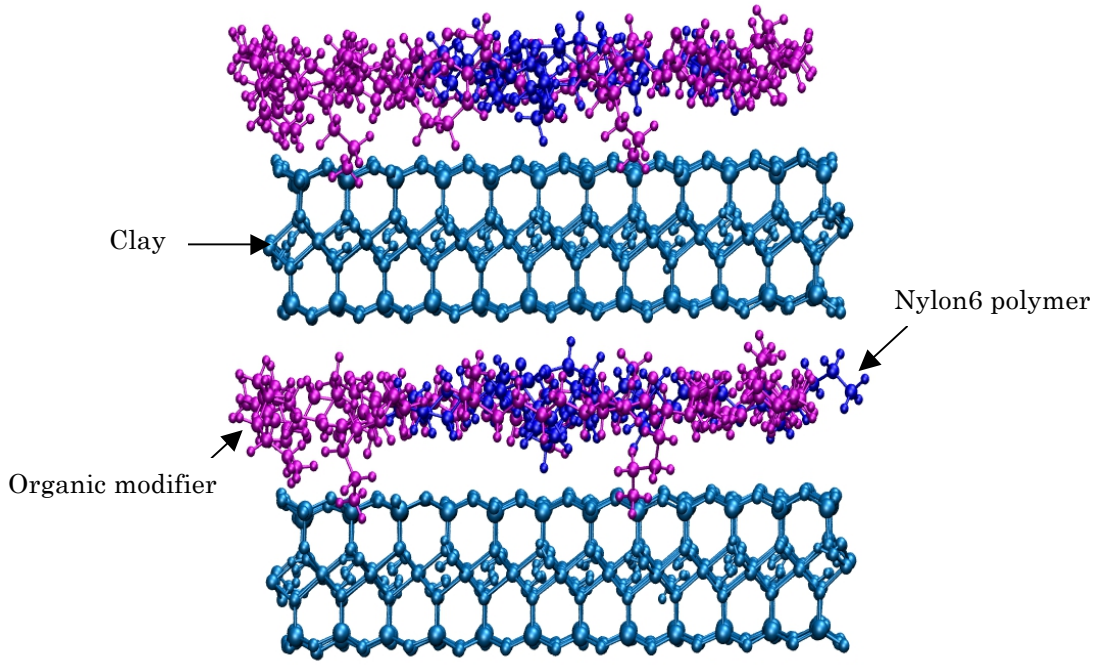

Figure 3.9. Final molecular conformation of Nylon6-PCN

First, non-bonded interaction between PBT-PCN constituents and Nylon6-PCN constituents were quantified. Interaction energy between clay and modifier is attractive and higher than the interaction energy between clay and polymer. Partial charges of individual atoms in modifiers are higher than the polymers thus leads to grater interaction. Interaction energies between clay and polymer are attractive and higher than the interaction energy between polymer and modifier. Following table shows the interaction energies.

Table 3.9. Interaction energies between PCNs constituents

Component of PCN	Electrostatic energy (kcal/mol) [Col-A]	van der Waals energy (kcal/mol) [Col-B]	Total non-bonded energy (kcal/mol) [Col-A + Col-B]
PBT-PCN			
Clay- Polymer	-36	-165	-201
Clay- modifier	-1836	-316	-2152
Polymer- Modifier	-93	-43	-136
Nylon6-PCN			
Clay- Polymer	12	-182	-170
Clay- modifier	-1464	-375	-1839
Polymer- Modifier	-209	-30	-239

Based on the table 3.10, the interaction energy between clay and modifier functional group is attractive and higher than the other constituents in both PCNs. This higher interaction between clay and modifier functional groups could be endorsed by higher positive partial charges in functional group atoms as shown in figure 3.1. Similarly, modifier backbone also has higher attractive interactions with clay compared to the polymer functional group and backbone in both PCNs. Polymer functional group has negative partial charges as shown in figure 3.1 thus it induces repulsive interaction with clay in both PCNs systems. Interaction energies between clay and individual atoms of organic modifier are shown in the table 3.11.

Table 3.10. Interaction energies between PCN components

Component of modifier, polymer and clay in PCN	Electrostatic energy (kcal/mol) [Col-A]	van der Waals energy (kcal/mol) [Col-B]	Total non-bonded energy (kcal/mol) [Col-A + Col-B]
PBT-PCN			
Clay-modifier backbone	-582	-282	-864
Clay-modifier functional group	-1255	-34	-1289
Clay-polymer backbone	-250	-108	-358
Clay-polymer functional group	+213	-56	+157
Nylon6-PCN			
Clay-modifier backbone	-485	-297	-782
Clay-modifier functional group	-979	-77	-1056
Clay-polymer backbone	-183	-123	-306
Clay-polymer functional group	+155	-62	+93

Table 3.11. Interaction energies between clay and modifier atoms

Individual atoms of organic modifiers and clay	Electrostatic energy (kcal/mol) [Col-A]	van der Waals energy (kcal/mol) [Col-B]	Total non-bonded energy (kcal/mol) [Col-A + Col-B]
PBT-PCN			
Clay-Modifier backbone hydrogen	-2512	-67	-2579
Clay-Modifier backbone carbon	+1930	-215	+1715
Clay-Modifier functional hydrogen	-2564	-7	-2571
Clay-Modifier functional nitrogen	+546	+37	+583
Clay-Modifier functional oxygen	+1628	-42	+1586
Clay-Modifier functional carbon	-865	-22	-887
Nylon6-PCN			
Clay-Modifier backbone hydrogen	-2085	-72	-2157
Clay-Modifier backbone carbon	+1600	-226	+1374
Clay-Modifier functional hydrogen	-2071	-7	-2078
Clay-Modifier functional nitrogen	+444	-2	+442
Clay-Modifier functional oxygen	+1359	-44	+1315
Clay-Modifier functional carbon	-711	-24	-735

It is observed that the organic modifier hydrogen atoms show higher magnitude of attractive interactions with clay as observed in the OMMT system. Interaction energies of individual polymer atoms with clay are shown in the following table.

Table 3.12. Interaction energies between clay and polymer atoms

Component of polymer and clay in PCN	Electrostatic energy (kcal/mol) [Col-A]	van der Waals energy (kcal/mol) [Col-B]	Total non-bonded energy (kcal/mol) [Col-A + Col-B]
PBT-PCN			
Clay-Polymer aromatic hydrogen	-301	-10	-311
Clay-Polymer backbone hydrogen	-380	-10	-390
Clay-Polymer aromatic carbon	+188	-59	+129
Clay-Polymer backbone carbon	+243	-29	+214
Clay-Polymer functional hydrogen	-90	-0.2	-90.2
Clay-Polymer functional oxygen	+1127	-36	1091
Clay-Polymer functional carbon	-824	-20	-844
Nylon6-PCN			
Clay-Polymer backbone hydrogen	-1056	-19	-1075
Clay-Polymer backbone carbon	+872	-104	+768
Clay-Polymer functional nitrogen	+593	-27	+566
Clay-Polymer functional hydrogen	-424	-2	-426
Clay-Polymer functional oxygen	+589	-13	+576
Clay-Polymer functional carbon	-600	-20	-620
Clay-Polymer backbone hydrogen	-1056	-19	-1075

Based on the results shown in the table 3.12, hydrogen and carbon atoms show attractive interaction with clay while the other atoms show repulsive interactions. Functional group carbon atoms contribute more attractive interactions and Oxygen atoms contribute more repulsive interactions. The greater negative partial charges of Oxygen atom induce greater repulsive interaction. As shown in the table 3.13, polymer backbone has higher repulsive interaction with modifier functional group and lesser repulsive interaction with modifier backbone. Polymer functional group has higher attractive interaction with modifier functional group and lesser attractive interaction with backbone. Similar nature of interactions has been reported in our previous work[5-8].

The non-bonded interactions play a major role in PCNs and they affect the crystallinity and mechanical properties of PCNs. Based on the results, more than 80%, 75%, 70% of interaction energies are result of electrostatic interaction for OMMT, PBT-

PCN and Nylon6-PCN respectively. Following figures show overall interaction energy map for PBT-PCN and Nylon6-PCN respectively.

Table 3.13. Interaction energies between modifier groups and polymer groups

Component of modifier and polymer in PCN	Electrostatic energy (kcal/mol) [Col-A]	van der Waals energy (kcal/mol) [Col-B]	Total non-bonded energy (kcal/mol) [Col-A + Col-B]
PBT-PCN			
Polymer backbone – modifier backbone	+115	-29	+86
Polymer backbone-modifier functional	+209	-10	+199
Polymer functional-modifier backbone	-132	-12	-144
Polymer functional-modifier functional	-285	+7	-278
Nylon6-PCN			
Polymer backbone – modifier backbone	+58	-20	+38
Polymer backbone-modifier functional	+91	-11	+80
Polymer functional-modifier backbone	-94	-11	-105
Polymer functional-modifier functional	-264	+11	-253

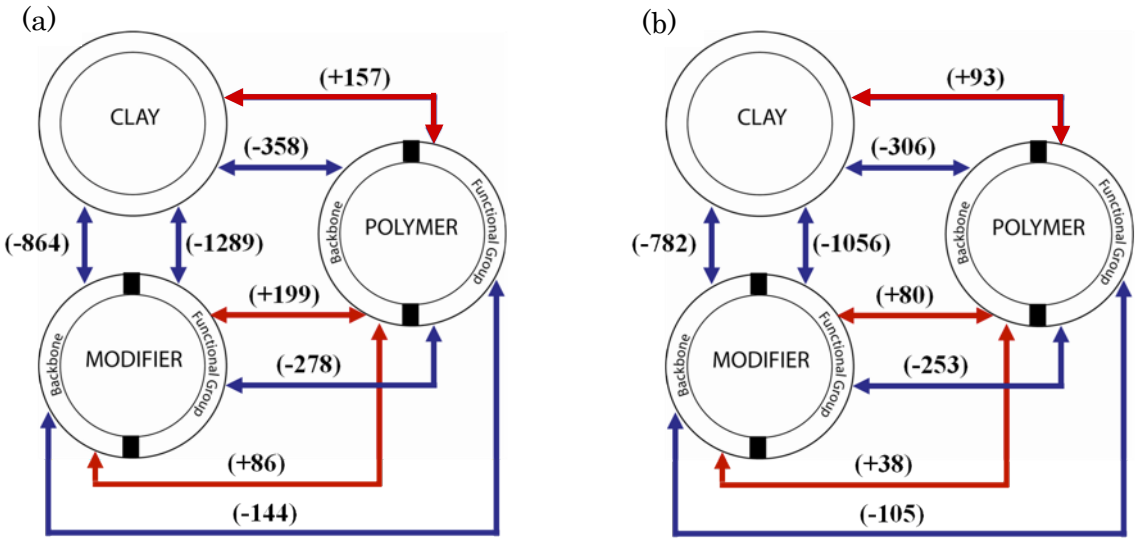

Figure 3.10. Interaction energy maps for (a) PBT-PCN and (b) Nylon6-PCN

The two energy maps have similar pattern in terms of attractive and repulsive interactions between different constituents of PCNs. These energy maps indicate that the PBT-PCN system has greater magnitude of interaction energies between different constituents than the Nylon6-PCN system.

In all three systems, OMMT, PBT-PCN and Nylon6-PCN, modifier shows attractive interactions with the clay. Further, in PBT-PCN system, modifiers have 17% higher attractive interactions with clay than in Nylon6-PCN system. Polymer has attractive interaction with clay and modifier in both systems. In terms of interaction energy magnitudes, almost equal interaction between polymer and clay is observed in both PCN systems. However, 75 % higher interaction between polymer and organic modifier is observed in Nylon6-PCN compared to PBT-PCN.

Previous work has shown that the molecular interactions between clay, modifier and polymer result in significant alteration of polymer crystallinity in PCN[5]. This is the basis of the altered phase theory to explain the significant improvement in elastic modulus and hardness of PCN as a result of addition of small amounts of well-dispersed clay nano particles in the polymer. The attractive interactions between functional groups of the polymer with the modifier and concurrent repulsive interaction between modifier and polymer backbone result in reduction of crystallinity of the surrounding polymer.

In PBT-PCN system reduction in crystallinity and improved elastic modulus and hardness of the PCN were observed. Similar phenomena of reduction in crystallinity and improved elastic modulus and hardness were observed in Nylon6-PCN[5]. The crystallinity of pure PBT is 35.6 % while the crystallinity of pure Nylon6 is 27.6 %. In the Nylon6-PCN system the reduction in crystallinity is 16.5 % while the reduction in crystallinity is 0.5 % in the PBT-PCN system. The improvement in elastic modulus and hardness values in Nylon6-PCN is 63 % and 42 % respectively with respect to pristine

Nylon6. However, the improvement in elastic modulus and hardness values in PBT-PCN is only 10 % and 23 % respectively with respect to pristine PBT. This results show that in the Nylon6-PCN system, the clay-modifier is significantly altered the crystallinity of polymer and improved the elastic modulus and hardness. However, the same clay-modifier is moderately changed the crystallinity of polymer, elastic modulus and hardness in the PBT-PCN system.

Based on the interaction energy maps for the two systems shown in figure 3.10, the mechanism of attractive interaction between functional group of the polymer and modifier and repulsive interaction between backbone of the polymer and modifier leading to the changes in polymer crystallinity is present. The comparison of interaction energy maps for the two PCNs shown in figure 3.10 reveals that the interaction energies between polymer and modifier, and polymer and clay are higher in the PBT-PCN system than in the Nylon6-PCN system. The attractive interaction energy and repulsive interaction energy between polymer and modifier are 422 kcal/mol and 285 kcal/mol in the PBT-PCN. However, the attractive and repulsive interaction energies in the Nylon6-PCN are 358 kcal/mol and 118 kcal/mol respectively. The attractive and repulsive interaction energies between clay and polymer are 157 kcal/mol and 358 kcal/mol in the PBT-PCN system. However, the attractive and repulsive interaction energies between clay and polymer in the Nylon6-PCN system are 93 kcal/mol and 306 kcal/mol.

This results show that the initial crystallinity of the polymer may have affected the magnitude of interaction energy needed to alter the crystallinity and improve the elastic modulus and hardness of the PCN. Thus, it appears that significantly higher interaction energies between clay-modifier and polymer may be required to alter the crystallinity and improve the elastic modulus and hardness of a polymer that is more crystalline to begin with.

References

1. Phillips, J. C.; Braun, R.; Wang, W.; Gumbart, J.; Tajkhorshid, E.; Villa, E.; Chipot, C.; Skeel, R. D.; Kalé, L.; Schulten, K. Journal of Computational Chemistry 2005, 26, (16), 1781-1802.
2. Humphrey, W.; Dalke, A.; Schulten, K. Journal of Molecular Graphics 1996, 14, (1), 33-38.
3. Cruz-Chu, E. R.; Ritz, T.; Siwy, Z. S.; Schulten, K. Faraday Discussions 2009, 143, 47-62.
4. Katti, D. R.; Katti, K. S.; Raviprasad, M.; Gu, C. J. Journal of Nanomaterials 2012.
5. Sikdar, D.; Katti, D.; Katti, K.; Mohanty, B. Journal of Applied Polymer Science 2007, 105, (2), 790-802.
6. Sikdar, D.; Katti, K. S.; Katti, D. R. Journal of Nanoscience and Nanotechnology 2008, 8, (4), 1638-1657.
7. Sikdar, D.; Katti, D. R.; Katti, K. S. Journal of Applied Polymer Science 2008, 107, (5), 3137-3148.
8. Sikdar, D.; Katti, D. R.; Katti, K. S.; Mohanty, B., International Journal of Nanotechnology, 2009; Vol. 6, pp 468-492.

DIFFUSION OF OXYGEN GAS IN POLYBUTYLENE TEREPHTHALATE

Introduction

A study of Oxygen gas diffusion in Polybutylene Terephthalate polymer (PBT) for the application of coatings by means of molecular dynamics simulation was conducted. Experimental study demonstrates improved elastic modulus and hardness in PBT nanocomposites than in pure PBT polymer[1]. Therefore, the primary approach was to understand the molecular mechanism of Oxygen gas diffusion in pure PBT polymer hence to enhance the barrier property of PBT or PBT nanocomposite. Diffusion mechanism at molecular level provides a better understanding thus enhancement of barrier property in polymeric system is viable. By using MD simulation, molecular system can be studied with different conditions such as temperature, pressure, polymer density, and polymer chain length, to investigate the dependence. The intention of this work is to explain the diffusion mechanism in terms of interactions between Oxygen and polymer, and polymer conformation by means of molecular dynamics simulation.

In this work, the absolute rate of Oxygen, Oxygen interaction with polymer and polymer conformation were investigated from the simulation results. Following sections explain molecular model construction, simulations, polymer conformations, interactions energy between Oxygen and polymer, absolute rate of Oxygen in detail.

Computational Methods

The Molecular Dynamics (MD) simulations and post processing analyses were performed using NAMD[2] and VMD[3] respectively. Materials Studio was used to construct molecular models and generate initial coordinates. The molecular structure information was obtained using TopoTools plug-in that is available in VMD. RMSD Trajectory Tool in the VMD was used to calculate the RMSD value of a molecule. Interaction energy between molecules was calculated using NAMD Energy module that is available in

VMD. Kinetic energy of a molecule was calculated using the script, which is described in the appendix. CHARMM[4] force field parameters were used for PBT polymer to represent the potentials. CHARMM model components with PET polymer[5] were used to obtain the force field parameters for PBT. For a molecular simulation study Oxygen molecule can be represented either two centers potential or one center potential. In this work, one center potential single atom with a sigma of 3.43 Å and well depth of 940 J/mol[6] was used to represent the Oxygen gas. The number of Oxygen molecules to be inserted in the model was calculated based on the relationship between pressure, volume and temperature[7]. All the simulations were performed using 16 numbers of 2.66 Ghz 5430 Penryn processors with one terabyte memory. The clock time for each simulation was 105253 seconds.

Initially, a molecular model of PBT monomer was generated and then coordinate, structure information were obtained using Materials Studio and VMD respectively. The figure 4.1 shows the molecular model of PBT unit. Here, blue color shows Carbon atom, red color shows Oxygen atom and light blue color shows Hydrogen atom. A single chain of polymer that consists of 326 atoms and end-to-end distance of 192 angstrom was constructed with twelve units. Selection of appropriate amount of polymer in a molecular system is crucial therefore four different amounts of polymer models were constructed. All four molecular models were subjected to the simulation protocol that explained in the following section.

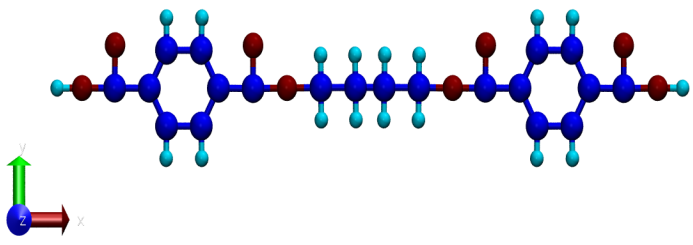

Figure 4.1. A molecular model of PBT unit

Table 4.1. Molecular model decription

Model	Number of polymer chains	Molecular mass (amu)
M_3	3	7765.68
M_6	6	15531.36
M_9	9	23297.04
M_{12}	12	31062.72

Importantly, a molecular model based on the measured density of PBT films was constructed in order to compare the results with other models. Density was measured from the PBT films that were prepared to investigate the mechanical properties experimentally[1]. The measured density is 1.1 g/cm^3 and the molecular model consists of 256 polymer chains that contain 83456 atoms. This model is defined as model M_{256}. Molecular models were minimized for sufficient time and the minimization was confirmed with the total potential energy and root mean square deviation of the molecules. In general, constant potential energy values and root mean square values are used to verify the minimized molecules. Based on these diagrams, it was verified that each model was minimized within five hundred time steps. The following diagrams show the potential energy variation and root mean square deviation of molecules for models M_3, M_6, M_9 and M_{12}.

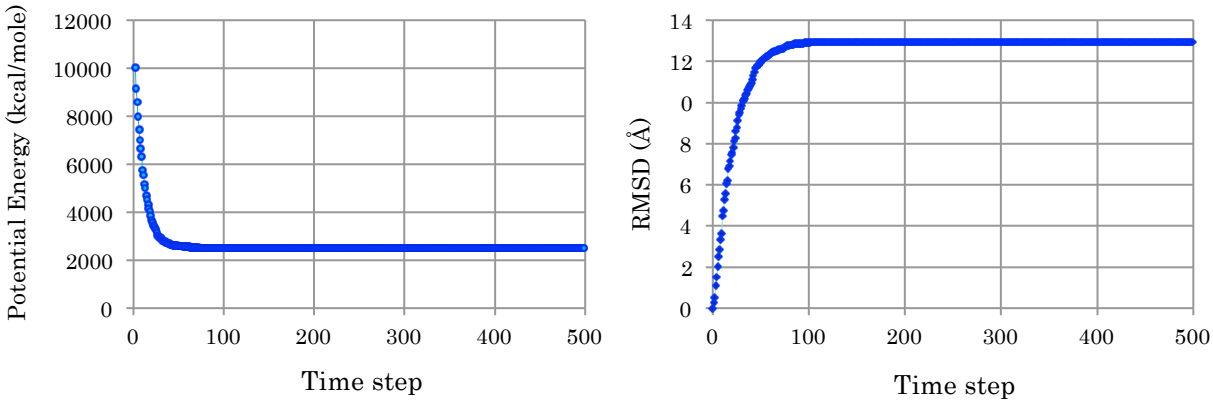

Figure 4.2. Potential energy variation and RMSD variation of model M_3

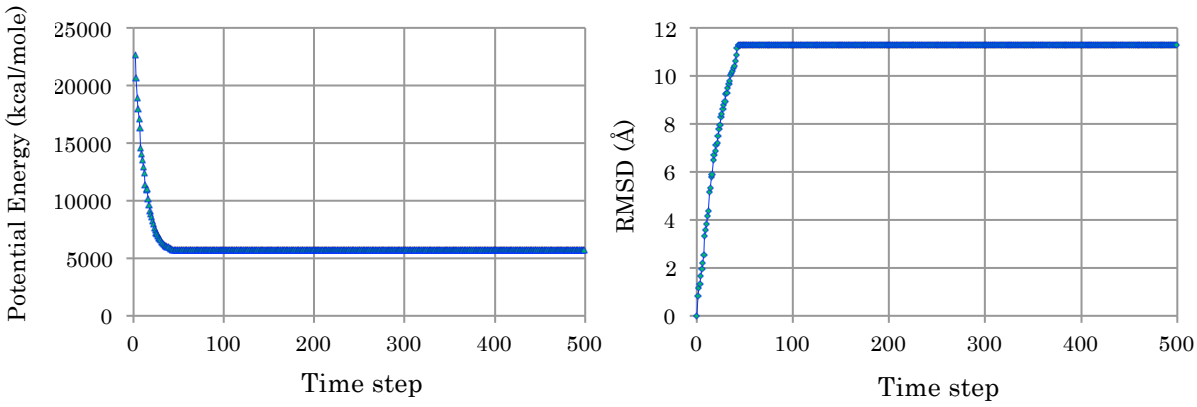

Figure 4.3. Potential energy variation and RMSD variation of model M_6

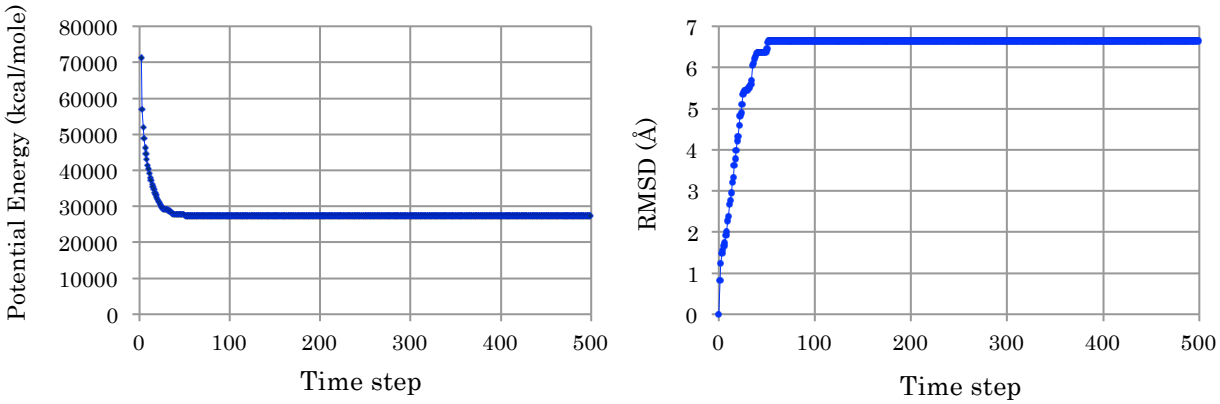

Figure 4.4. Potential energy variation and RMSD variation of model M_9

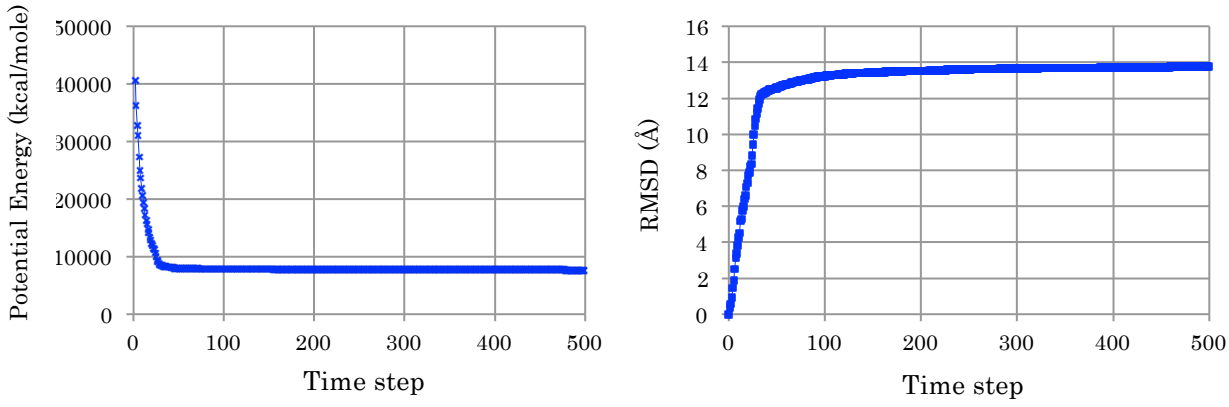

Figure 4.5. Potential energy variation and RMSD variation of model M_{12}

Molecular models were subjected to temperature increment in three equal steps up to 300 K using Langevin temperature control method after the minimization. Once the temperature reached 300 K, pressure was increased to atmospheric pressure in four equal steps using Langevin piston pressure method. Further, the models were subjected to temperature increment of 33 K and subsequently lowered the temperature by 33 K. The last step of temperature increment was performed to mimic the experimental condition[1]. Finally, models M_3, M_6, M_9 were simulated for 0.1 ns and M_{12} was simulated for 0.5 ns. However, model M_{256} was simulated for 1 ns. Once the equilibration of models was confirmed with root mean square deviation, polymer conformational changes in models M_3, M_6, M_9, M_{12} was compared with model M_{256} polymer conformational change visually.

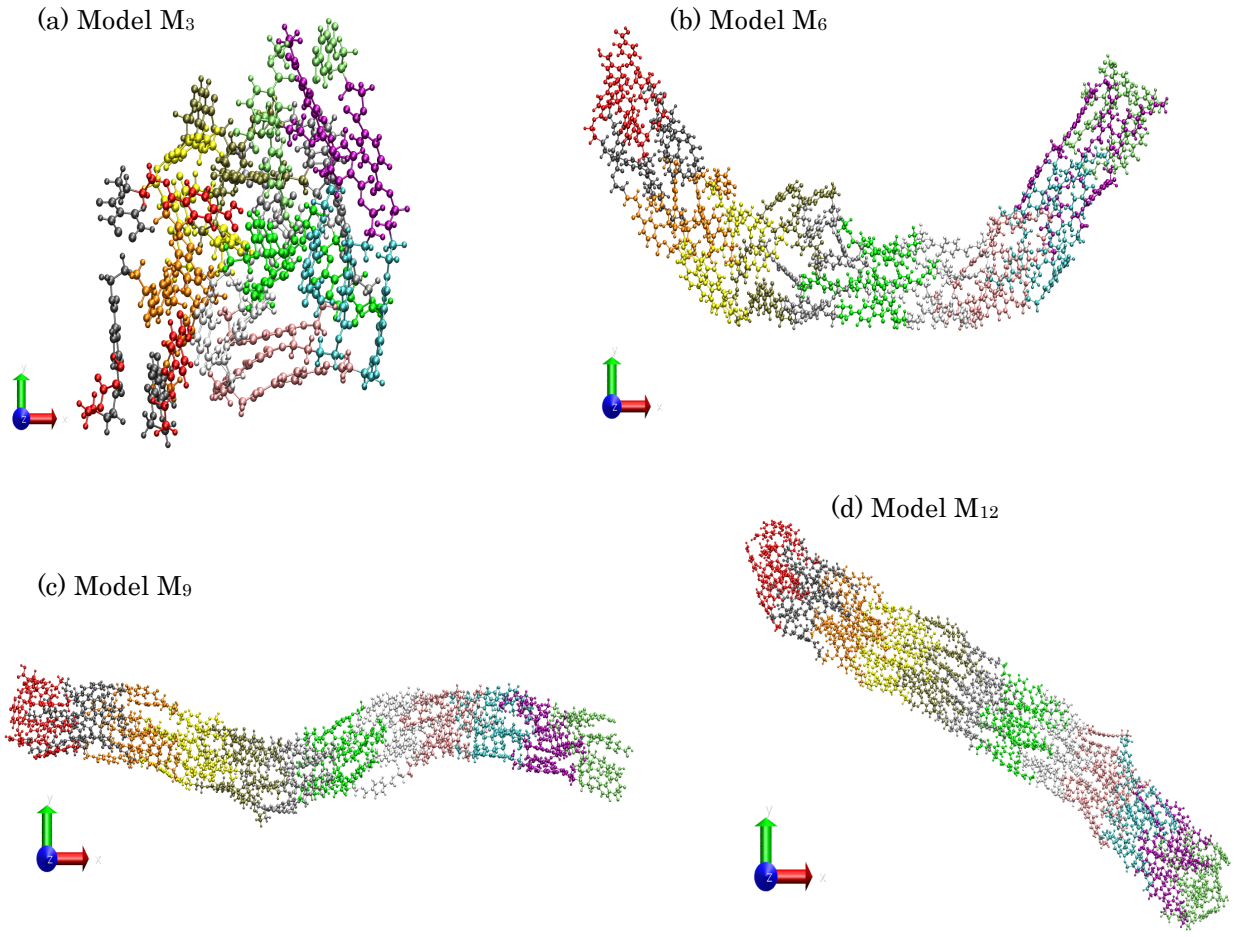

Figure 4.6. Conformational change of polymers

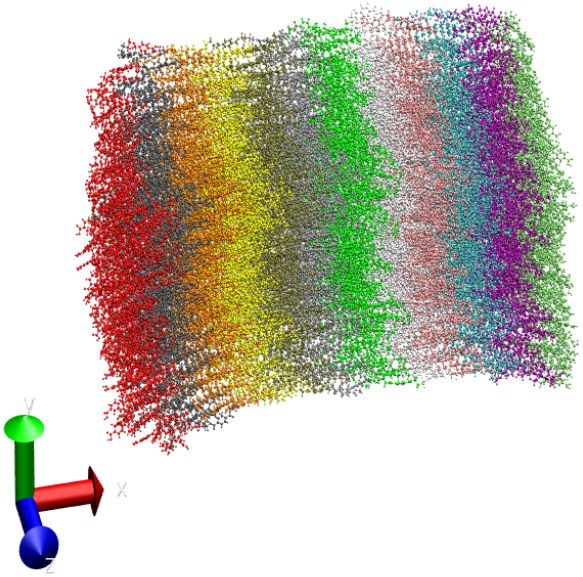

Figure 4.7. Polymer conformation of model M_{256}

Finally, one Oxygen molecule was introduced in the M_3, M_6, M_9, M_{12} simulation boxes and the simulations were performed for 5 ns. However, M_{256} was simulated with twenty-five Oxygen molecules, which are inserted randomly into the model. All the simulations were done under NPT conditions, which are constant number, pressure and temperature. For all simulations, 0.5 fs integration time and 12 Å cutoff distance with a switch distance of 10 Å was used.

Diffusion coefficient of a small particle in suspended liquid can be calculated using the Einstein's relationship[8]:

$$\langle |r(t) - r(0)|^2 \rangle = 6Dt \quad \rightarrow (1)$$

Where $\langle |r(t) - r(0)|^2 \rangle$ is the average mean square displacement of a penetrant at a time t with respect to original position, D is the diffusion coefficient of a penetrant. This equation is mainly used to calculate the diffusion coefficient in suspended liquid system or gas system[8] however polymer system is neither suspended liquid nor gas. Further,

equation 1 is the standard method to quantify the diffusion coefficient in polymeric system. However, I was interested in calculating coefficient based on the penetrants absolute displacement that could reveal the rate of change of the Oxygen's position in the polymer. The similar method was adapted as the absolute rate theory to study the molecular migration in condensed phase using Fick's law[9]. I believe that absolute rate of Oxygen in a polymeric system is an appropriate measure to be considered in order to quantify the Oxygen's movement in PBT polymer. Therefore, coefficient was calculated based on Oxygen's absolute displacement, which is described in the following equation:

$$|S(t+1) - S(t)| = Rt \quad \rightarrow (2)$$

Where $|S(t+1) - S(t)|$ is the absolute displacement of a penetrant at a time t, R is the rate of change of a penetrant's position. Figure 4.8 delineates both mean square displacement and absolute displacement calculation approaches.

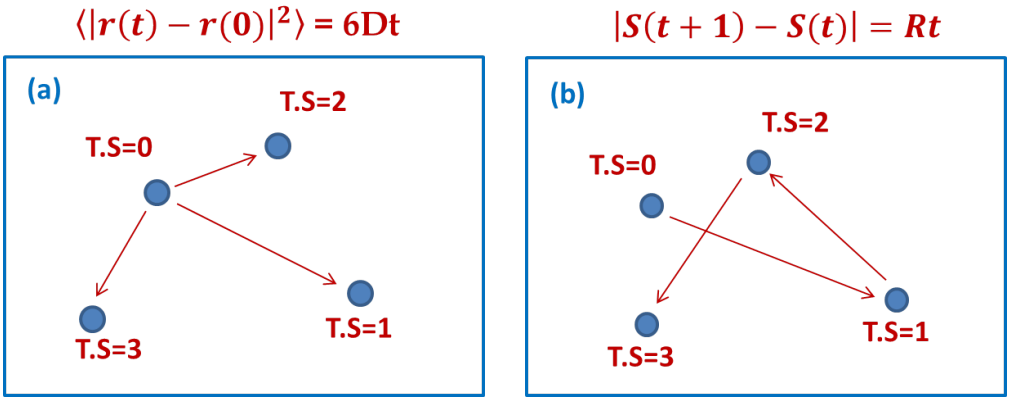

Figure 4.8. Pictorial representation for a displacement calculation of Oxygen molecule

"A Process of diffusion, which is to be looked upon as a result of the irregular movement of the particles produced by the thermal molecular movement"[8] was considered in deriving the diffusion coefficient. Therefore, it is crucial to consider the thermal molecular movement that induces interaction between penetrant, Oxygen molecule, and polymer. As explained earlier one-centered potential for Oxygen gas was

used that induces Van der Waals interaction with polymer. Therefore, Van der Waals interaction energy between Oxygen molecule and PBT polymer was investigated.

Results and Discussion

In this section, model M_{12A} simulation results are presented in detail. Further, Oxygen's movement in polymer and diffusion mechanisms in terms of interaction energy and polymer conformation is discussed. First, the Oxygen molecule position was observed visually during the 5 ns period in the models M_3, M_6, M_9 and M_{12}. This visual inspection unveils that the Oxygen molecule moved within the simulation box however never diffused into the polymer system during the entire simulation. This phenomenon happens because of the polymer conformation. The conformation of polymer shields the Oxygen molecule entering into the polymer.

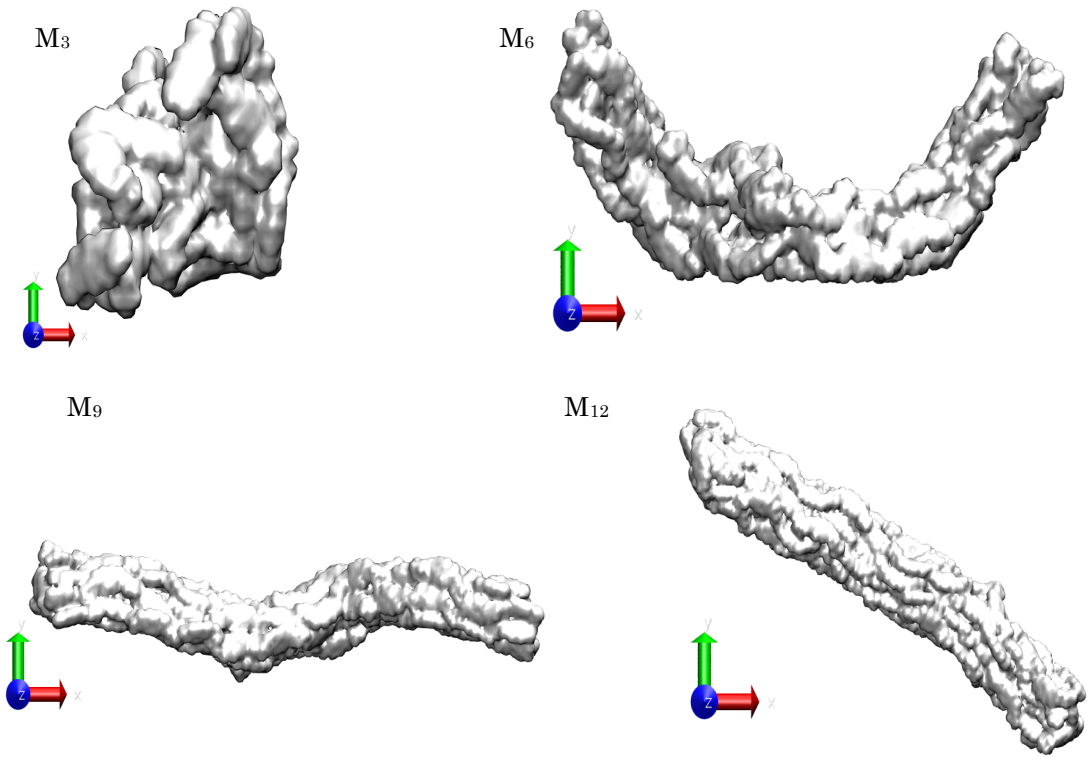

Figure 4.9. Volume map of molecular models

Secondly, conformational changes of polymer in model M_{12} was compared with conformational changes of polymer in model M_{256}. This conformational comparison was used to select the applicable size of the molecular model. Conformational comparison shows that model M_{12} has similar conformation as in model M_{256}. Therefore, a new model was built, which is defined as model M_{12A} shown in figure 4.10, by arranging twelve-polymer chains orderly and placing an Oxygen molecule at the center of the polymer chains.

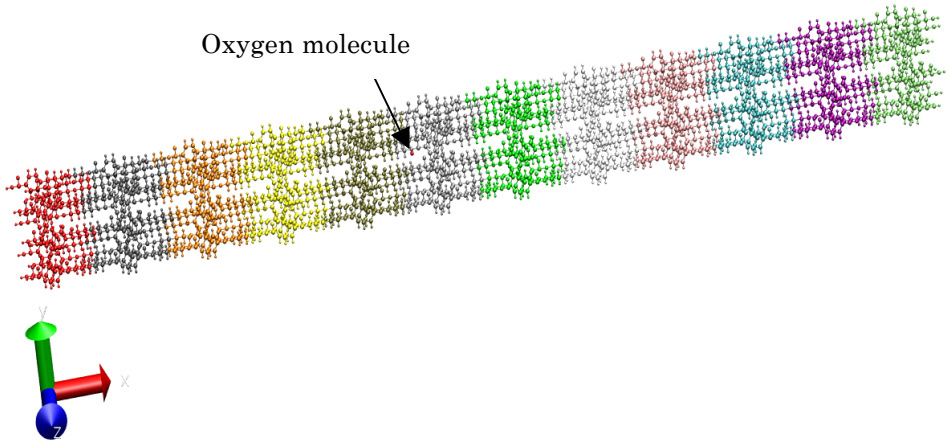

Figure 4.10. Initial molecular model M_{12A}

This model was subjected to the simulation protocol that was explained above and the simulation was performed for 3 nanoseconds. As mentioned earlier, polymer conformation is an important factor therefore model M_{12A} was simulated under two different conditions. These two simulations were performed purely to evaluate the importance of the conformation of polymer. In the first simulation, polymer constraint in all three directions; which means conformational changes of polymer is very minimal however Oxygen molecule was allowed to move freely within the polymer. In the second simulation, polymer and Oxygen atom were allowed to move freely. These conditions were adjusted in the molecular simulation input file. First, conformational change of

polymer for these two simulations was observed visually. Visual presentation as shown in the figure 4.11 clearly indicates that the importance of the polymer conformation.

(a) Conformational changes of polymer in the “Polymer Constraint”

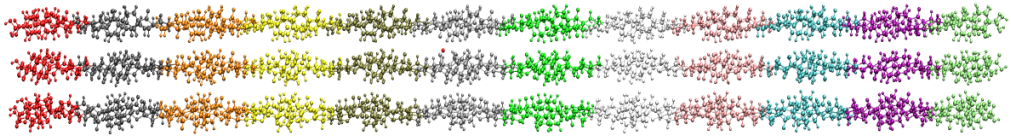

(b) Conformational changes of polymer in the “Polymer not constraint”

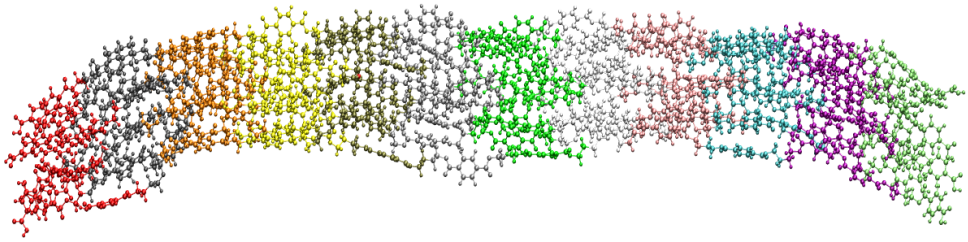

Figure 4.11. Conformational changes of polymer

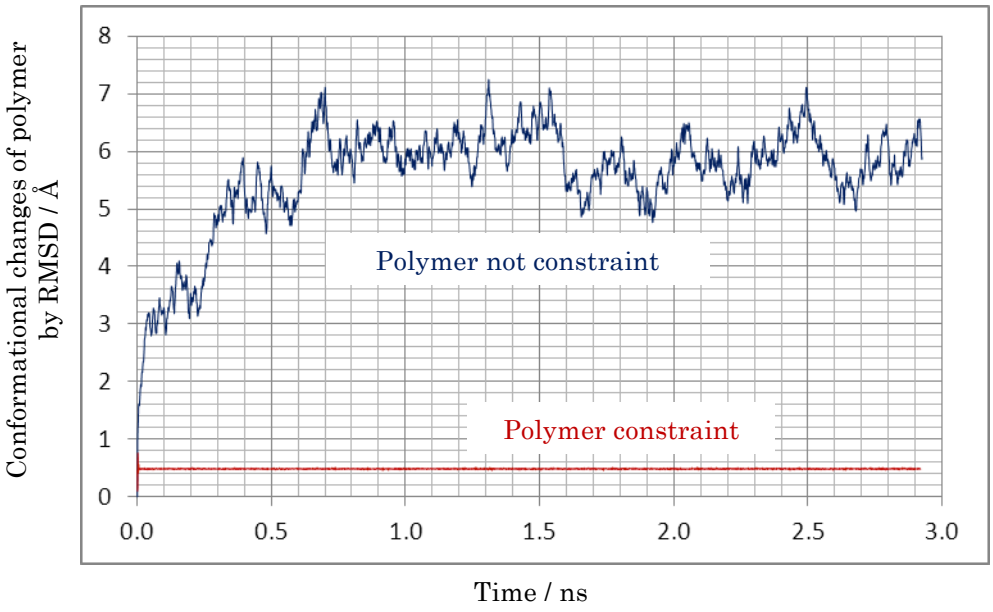

Figure 4.12. Conformational changes of polymer by Root Mean Square Deviation

The conformational change of polymer was calculated using root mean square deviation. This calculation provides clear measure for the conformational changes in polymer. Figure 4.12 shows the conformational changes of polymer quantitatively. The Oxygen gas movement for these two simulations was evaluated using RMSD. Figure 4.13 shows the movement of Oxygen molecule in the polymer for these two conditions. Results show that the Oxygen molecule stays in the polymer in the case of "polymer constraint" simulation however Oxygen molecule diffuses within the polymer in the case of "polymer not constraint" simulation.

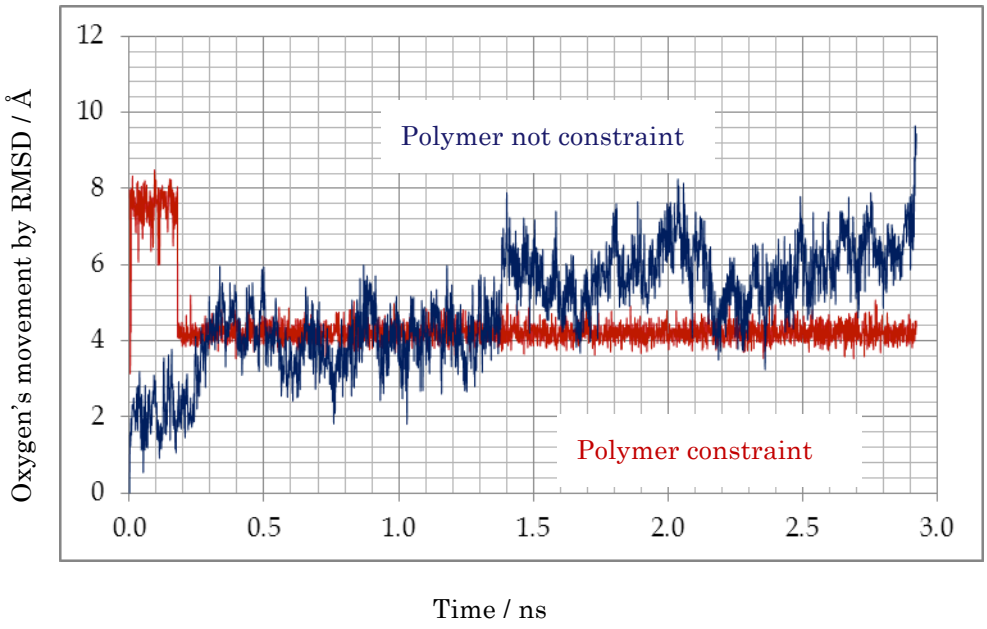

Figure 4.13. Oxygen's movement in polymer by Root Mean Square Deviation

Oxygen molecule is subjected to kinetic energy and Van der Waals energy during the molecular simulation. Both of these energies for "polymer not constraint" and "polymer constraint" simulations were evaluated and the results are shown in figure 4.14 and figure 4.15. The average kinetic energy of the Oxygen in both conditions is similar however Van der Waals energy between Oxygen and polymer is much greater in

"polymer not constraint" condition than in "polymer constraint" condition. These results infer the importance of the polymer conformation during the diffusion process.

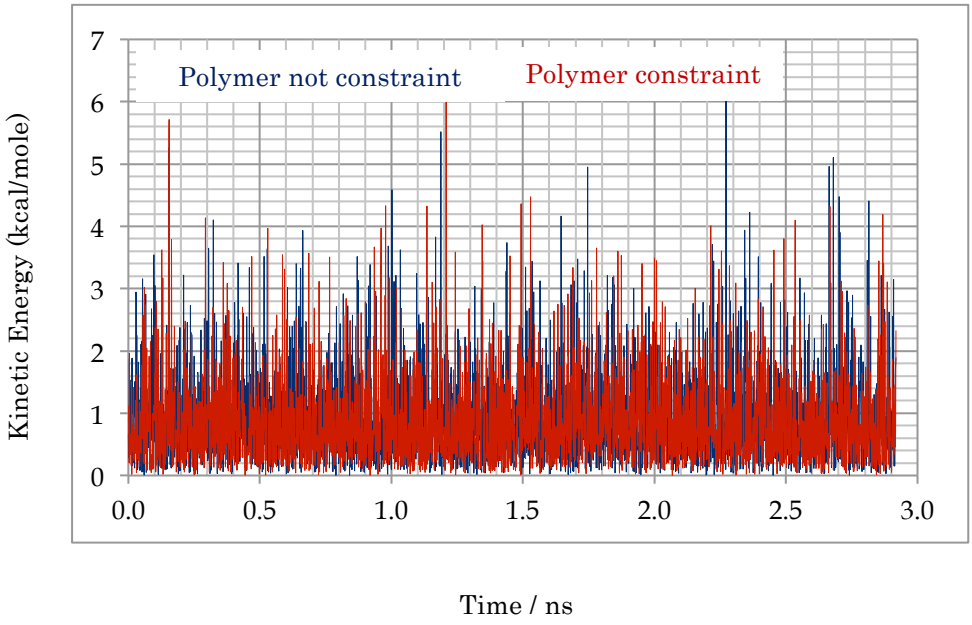

Figure 4.14. Kinetic energy variation of Oxygen molecule

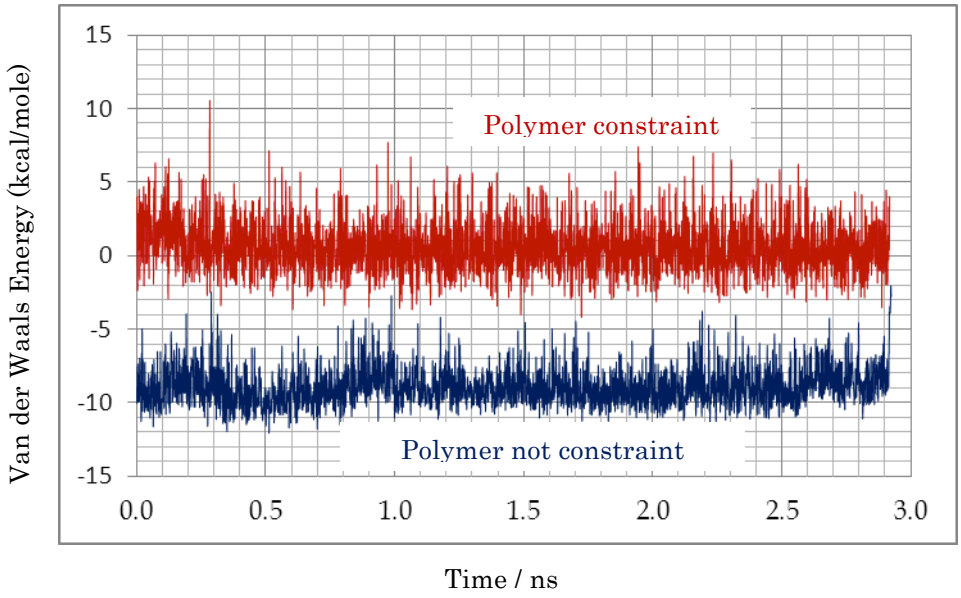

Figure 4.15. Van der Waals energy between Oxygen and polymer

As mentioned earlier, model M_{12A} was simulated for 3 ns however in this work I was

interested in the simulation time when Oxygen atom moved within the polymer. Therefore the MSD plot is drawn for 2.92 ns.

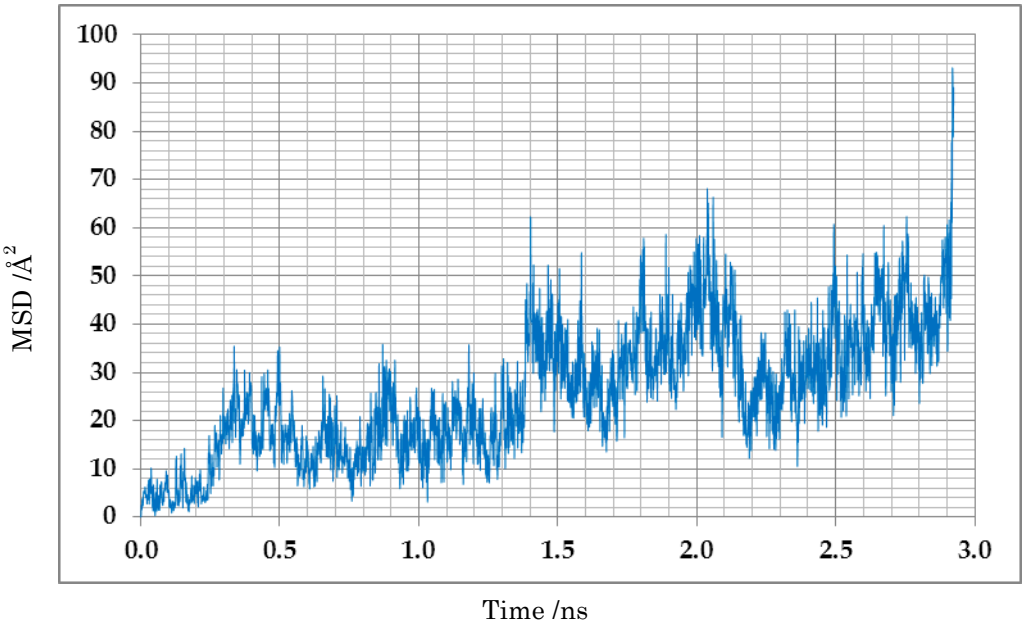

Figure 4.16. Mean square deviation of the Oxygen molecule

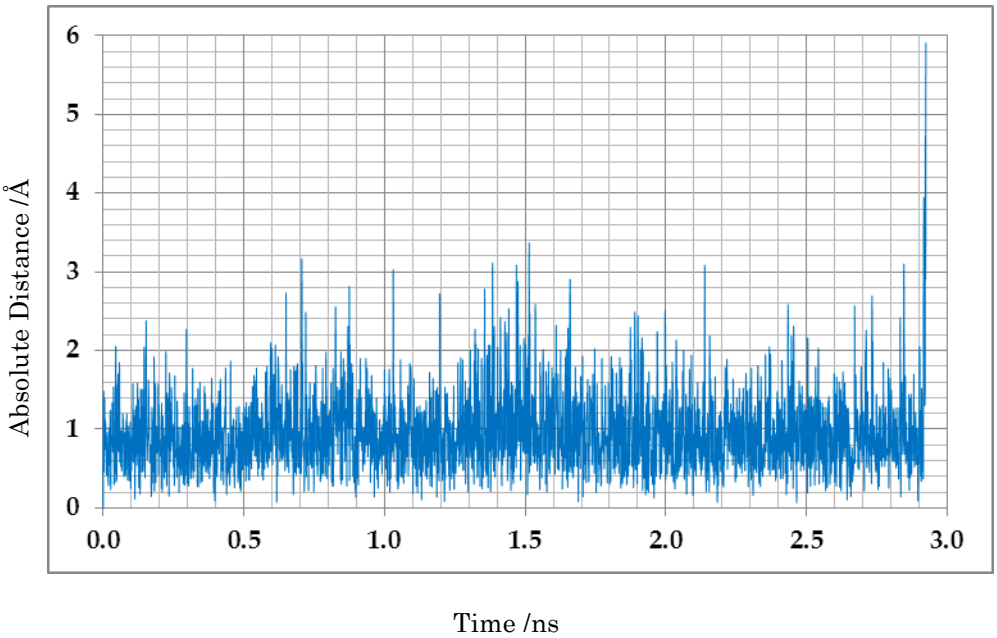

Figure 4.17. Absolute displacement variation of the Oxygen molecule

The mean square displacement and absolute displacement at each time step for model M_{12A} were calculated at temperature 300 K using equation-1 and equation -2. Both mean square displacement and absolute displacement variations are shown in above figures. Based on the equation 1 it is important to quantify the diffusion coefficient by means of liner fit of the MSD values. However in this work simulation time is very short thus calculation of the diffusion coefficient based on the plot shown in the figure 4.18 is $1.62*10^{-10}$ m^2/s.

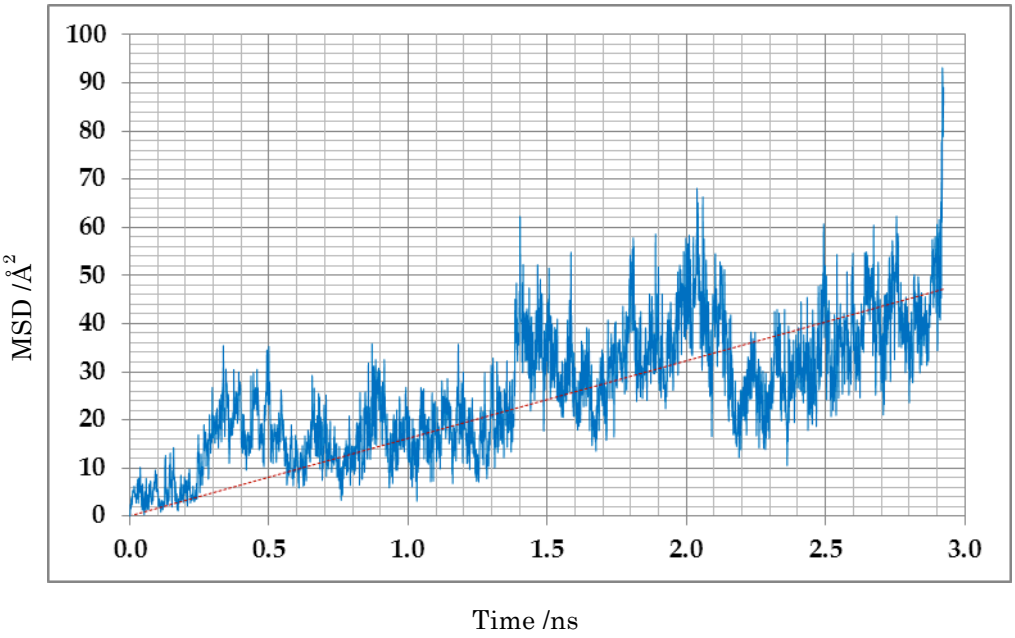

Figure 4.18. Mean square deviation of the Oxygen molecule with linear fit

Further, the absolute rate of Oxygen molecule in PBT polymer was quantified from the cumulative absolute displacement variation with simulation time as shown in the figure 4.19. The quantified absolute rate of Oxygen in PBT polymer is 95 m/s. Based on the simulation results, which is shown in the figure 4.17, maximum absolute displacement of the Oxygen is 3.36 angstrom however average absolute displacement of the Oxygen in PBT polymer is 0.92 angstrom. Further, Oxygen atom traveled 2724 angstrom for 2.92 ns of simulation time.

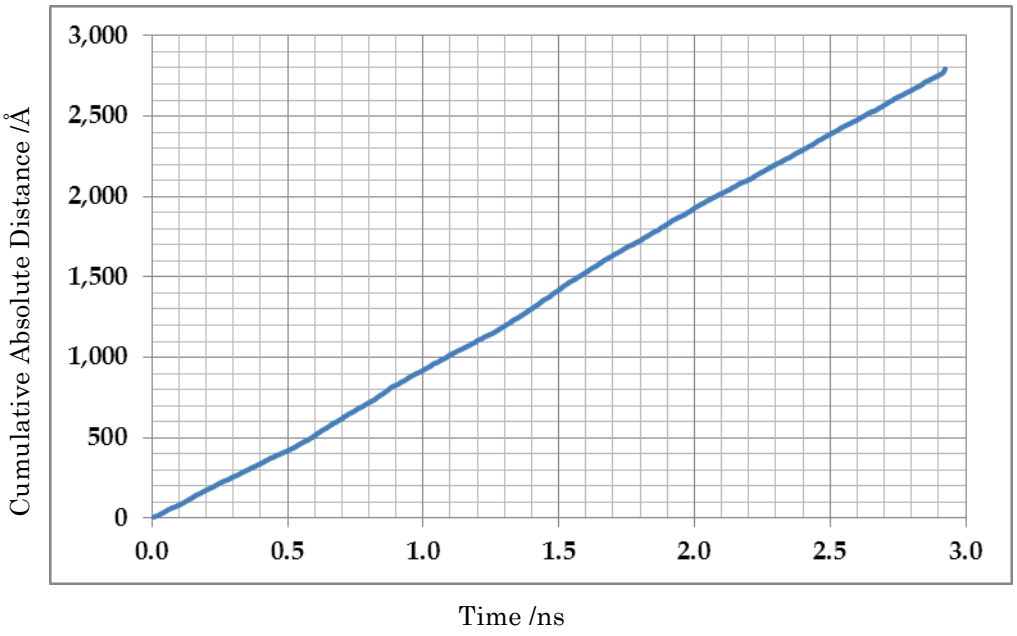

Figure 4.19. Cumulative absolute displacement of the Oxygen molecule

As mentioned earlier, Oxygen molecule is subjected to kinetic energy and Van der Waals energy. The polymer, which is selected for the Van der Waals interaction energy calculation and local conformational changes evaluation, is based on the Oxygen's trace during the simulation as shown below.

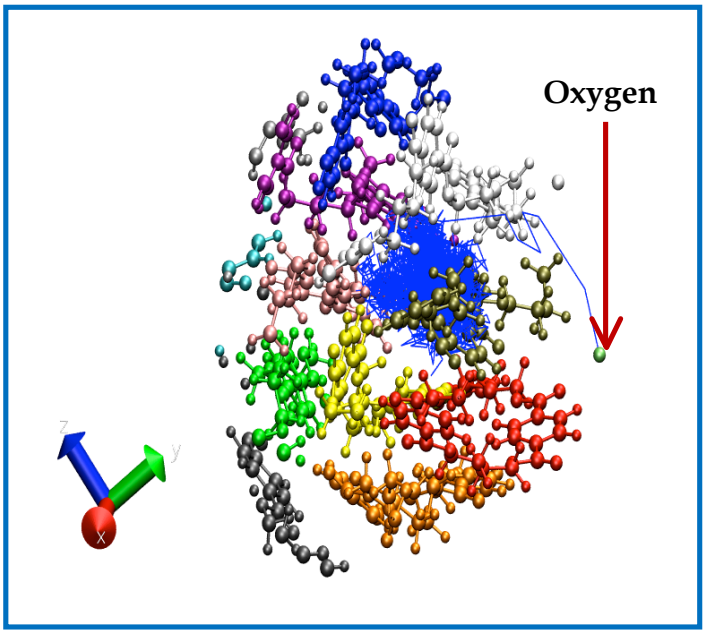

Figure 4.20. PBT polymer with Oxygen's trace during the simulation

Interactions and polymer conformation for different amounts of polymer with respect to Oxygen's position during the simulation was calculated. This analysis was done to study the influence of amount of polymer on the interaction and polymer conformation. These polymers were considered based on the Oxygen's position in the polymer. In this analysis 5 Å, 7 Å and 10 Å radius of volume of polymer was considered. Figure 4.21 shows the schematic representation of Oxygen's position.

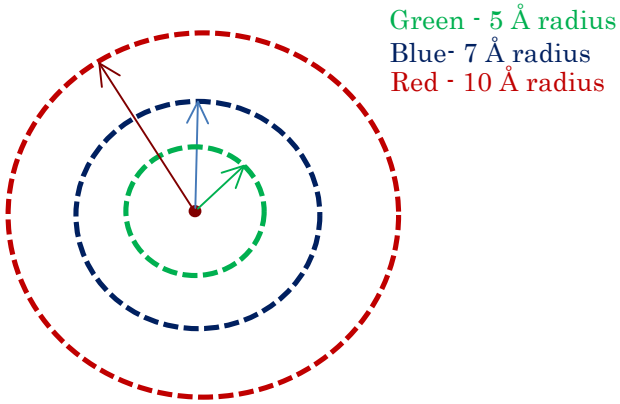

Figure 4.21. Schematic representation of different distances from Oxygen molecule

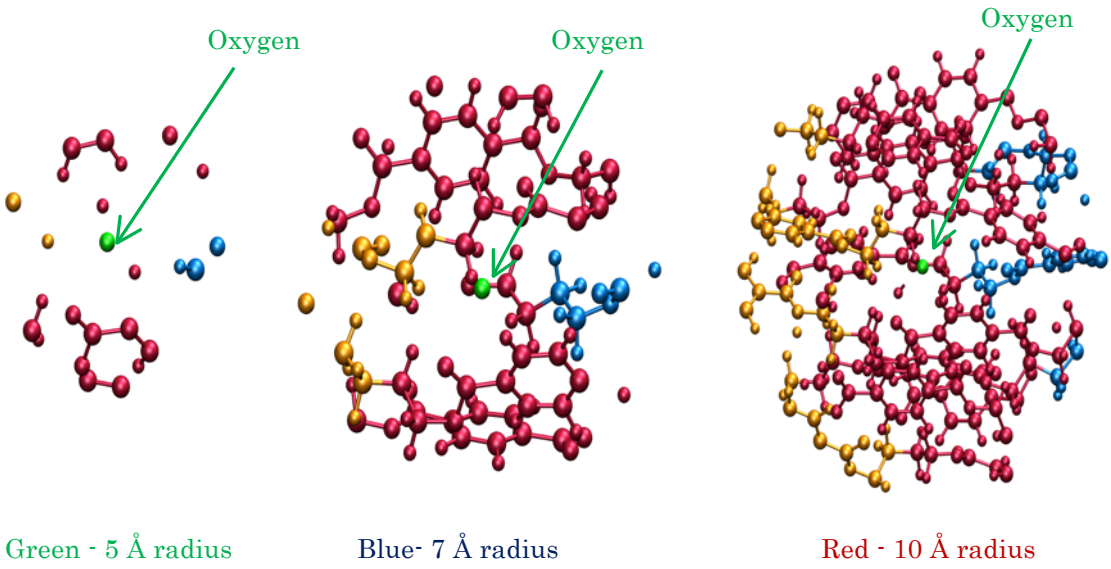

Figure 4.22. Visual representation of atom counts at different distances

First, polymer conformation for these three different conditions was evaluated. Result shows that polymer conformation does not change based on the polymer amount. This reveals that change in polymer conformation occurs very close to the Oxygen molecule. The figure 4.23 shows the polymer conformations quantitatively.

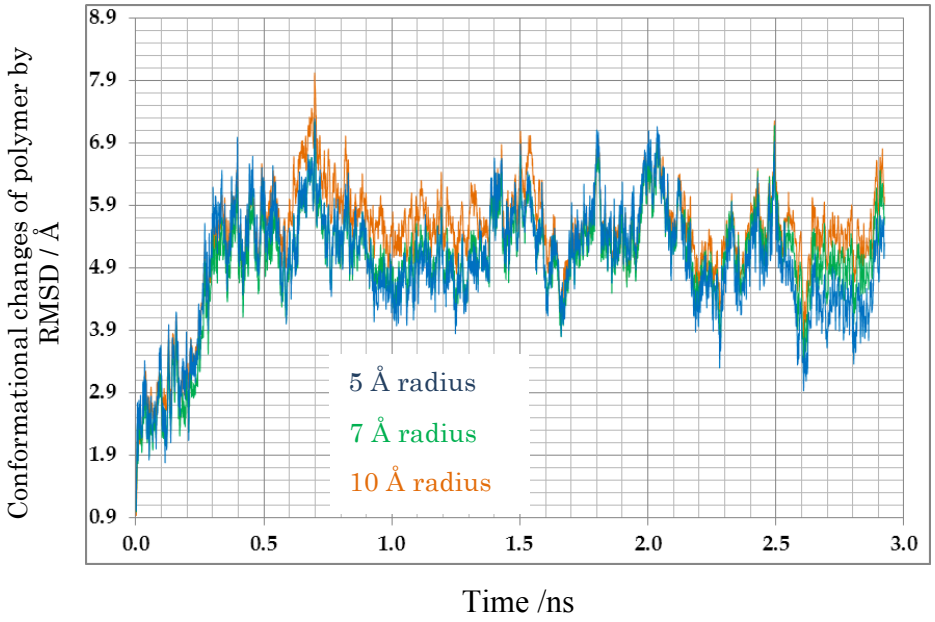

Figure 4.23. Conformational changes of polymer at different distances from Oxygen

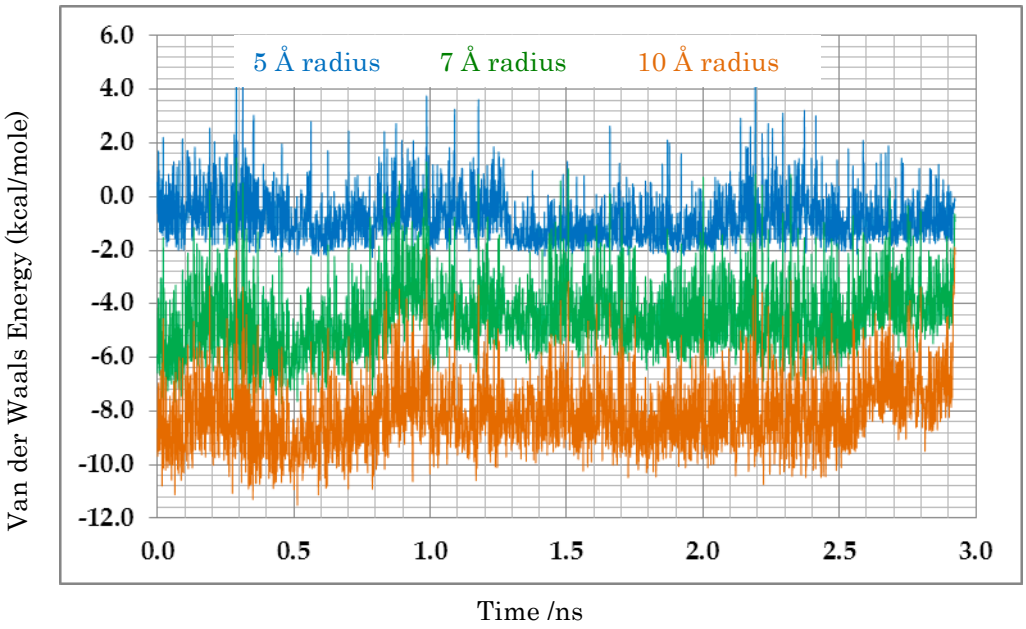

Figure 4.24. Van der Waals interaction between Oxygen and polymer

Interaction energy between Oxygen and polymer for these three conditions was evaluated. Figure 4.24 shows the interaction energy between Oxygen molecule and polymers. It is clear that Oxygen molecule is subjected to less Van der Waals interaction when 5 Å radius of volume of polymer is considered. This is because there are few numbers of atoms in the 5 Å radius of volume of polymer compared to the 10 Å radius of volume of polymer. The magnitudes of the interactions vary based on the amount of polymer however the interaction patterns are similar in all three conditions. We analyzed four different time periods to study the interaction pattern closely. Figure 4.25 shows the interaction pattern. This analysis indicates that interaction pattern does not change with the number of polymer atoms. These results validate the polymer conformation, which is similar in all three conditions.

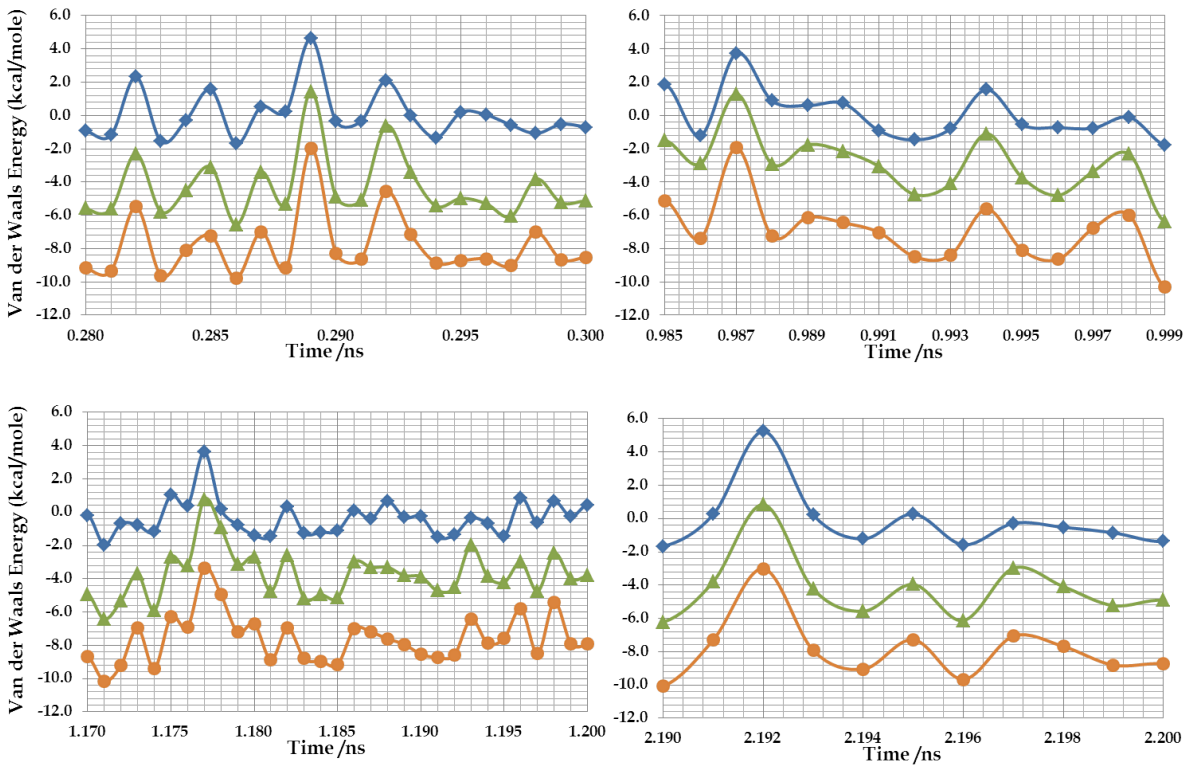

Figure 4.25. Van der Waals inetraction energy variation for short period of time

The variation of overall attractive interaction energy between Oxygen molecule and polymer, and kinetic energy of Oxygen molecule are shown in figure 4.26. The average Van der Waals energy varies from 10 kcal/mole to 8.8 kcal/mole however, attractive interaction energy fluctuates between 2.47 kcal/mole and 11.4 kcal/mole. The maximum kinetic energy of the Oxygen molecule is 6.495 kcal/mole however the average kinetic energy is 0.9 kcal/mole.

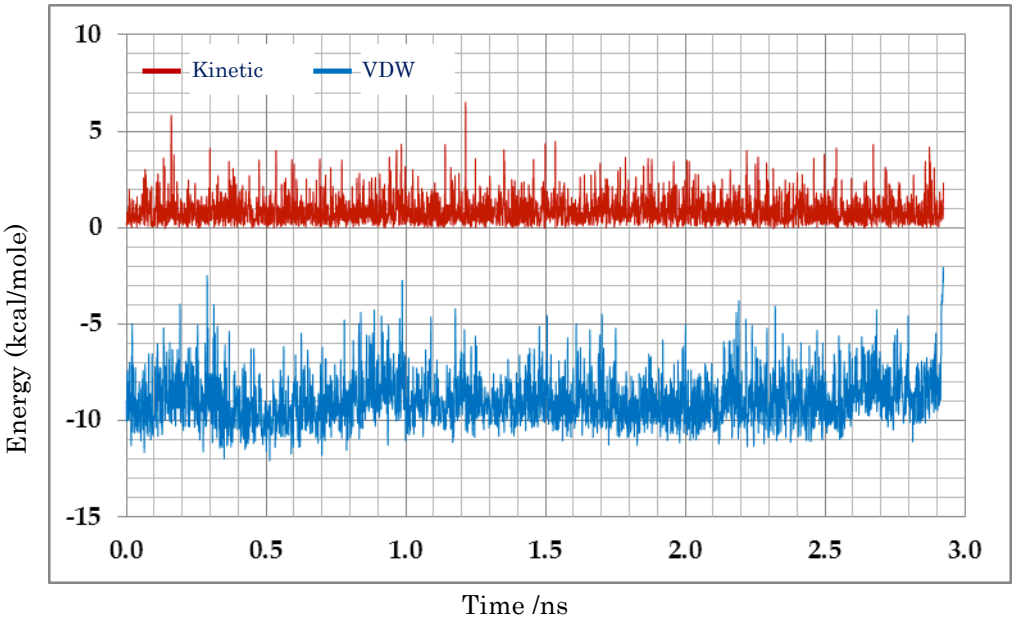

Figure 4.26. Van der Waals and kinetic energy of the Oxygen molecule

Root mean square deviation (RMSD) of polymer was used to evaluate the local conformational changes in polymer in the presence of Oxygen molecule. The local conformational change of pure polymer and polymer with Oxygen molecule was evaluated thoroughly and the result is shown in figure 4.27. Three simulations were performed in the case of pure polymer in order to study the influence of Oxygen molecule in the polymer conformation. It is observed from the results that conformation of polymer changes over a time in both pure polymer and polymer with Oxygen molecule however polymer with Oxygen molecule shows significant change in polymer

conformation compared to pure polymer conformation. Further, when Oxygen molecule moved from the polymer system conformational changes of polymer shows similar conformation as in the pure polymer.

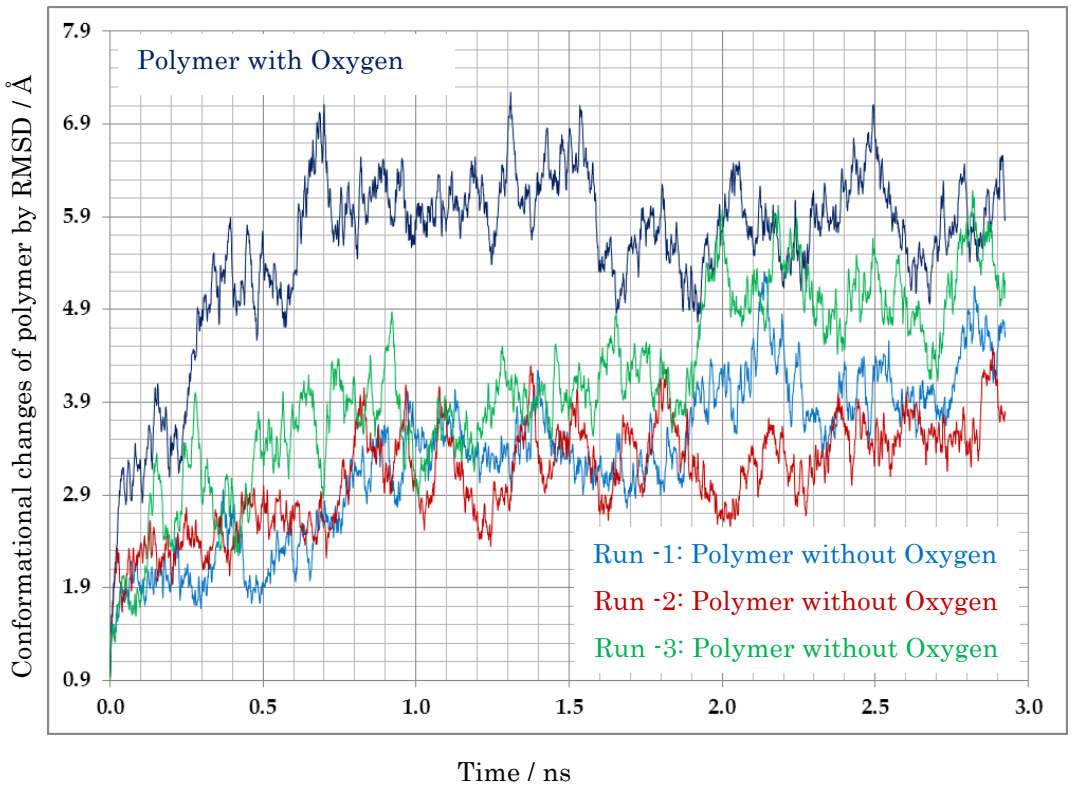

Figure 4.27. Local conformational changes of polymer

Random time intervals were selected to investigate the local conformational changes of polymer during the Oxygen's movement. Figure 4.28 shows the evolution of conformational changes at a random time interval. This evolution diagram clearly shows that the polymer conformation is changing locally when Oxygen molecule moves from one point to another. Results show that the conformational change of polymer aided Oxygen molecule to diffuse within polymer moreover presence of Oxygen molecule is also contributed to the conformational changes of polymer.

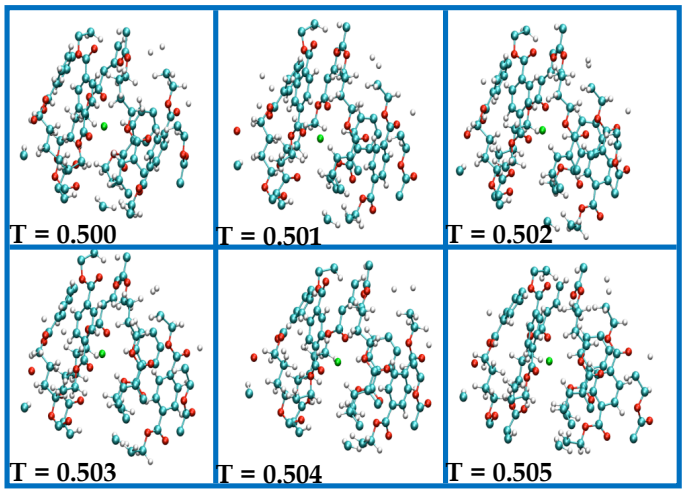

Figure 4.28. Visual representation of the Oxygen's movement in the polymer

Polymer conformation, interaction energy and absolute displacement were evaluated at every time step. First, Oxygen molecule movement was traced at a random time interval and corresponding absolute displacement, interaction energy, and conformation changes of polymer. This analysis clearly indicates that Oxygen molecule is subjected to significant change in absolute displacement, change in interaction energy with polymer and also change in polymer conformation when it moves from one point to another. For instance, when Oxygen molecule moved from time 0.500 ns to 0.501 ns, absolute displacement changed from 0.795 angstrom to 0.962 angstrom and attractive interaction energy changed from 9.1 kcal/mole to 11.5 kcal/mole and also polymer conformation changed from 5.62 angstrom to 5.505 angstrom. It should be noted that these absolute displacement values are contribution for overall diffusion process. Further, when Oxygen molecule moved from one point to another interaction energy difference is 2.4 kcal/mole and the magnitude is in the range of single hydrogen bond energy[10]. At molecular level this amount of interaction energy is significant contribution to the diffusion process. In molecular diffusion process Oxygen molecule diffuses with a help of both significant conformational changes of polymer and significant interaction

energy between Oxygen molecule and polymer. However, this is not the only scenario Oxygen can diffuse within polymer. For example, based on the figure 4.13, Oxygen molecule jumped from one point to another with insignificant change in polymer conformation however with greater interaction between Oxygen and polymer. In this case Oxygen molecule moved by 3.924 angstrom from 5.183 kcal/mole attractive interaction to 0.659 kcal/mole attractive interactions. At the same time, kinetic energy of Oxygen molecule changed from 0.167 kcal/mole to 0.882-kcal/mole and polymer conformation by RMSD value changed form 0.494 to 0.492. Based on this result it is clear that Oxygen molecule moves with greater interaction with polymer and kinetic energy however with minimal polymer conformation.

Based on the results obtained from the simulation I summarize that change of polymer conformation aids the Oxygen molecule to diffuse and further presence of Oxygen molecule influences the polymer conformation. The absolute rate of Oxygen in PBT polymer provides overall coefficient based on absolute displacement traveled by the Oxygen molecule. Van der Waals interaction energy between Oxygen molecule and polymer is evaluated and the result clearly indicates that Oxygen molecule is subjected to significant interaction with polymer when it moves from one point to another. Based on this study it confirms that Oxygen molecule has significant change in its absolute traveled displacement correspondingly significant change in interaction energies between Oxygen molecule and polymer, and change in polymer conformation.

References

1 Katti, D. R., Katti, K. S., Raviprasad, M. & Gu, C. Journal of nanomaterials, (2012).

2 Phillips, J. C.; Braun, R.; Wang, W.; Gumbart, J.; Tajkhorshid, E.; Villa, E.; Chipot, C.; Skeel, R. D.; Kalé, L.; Schulten, K. Journal of Computational Chemistry **2005,** 26, (16), 1781-1802.

3. Humphrey, W.; Dalke, A.; Schulten, K. Journal of Molecular Graphics **1996,** 14, (1), 33-38.

4. Brooks, B. R.; Bruccoleri, R. E.; Olafson, B. D.; States, D. J.; Swaminathan, S.; Karplus, M. Journal of Computational Chemistry **1983,** 4, (2), 187-217.
5. Cruz-Chu, E. R.; Ritz, T.; Siwy, Z. S.; Schulten, K. Faraday Discussions **2009,** 143, 47-62.
6. Hirschfelder, J. O.; Curtiss, C. F.; Bird, R. B., Molecular Theory of Gases and Liquids In Wiley: New York, 1954; p P.1111.
7. Neyertz, S.; Brown, D. Macromolecules **2008,** 41, (7), 2711-2721.
8. Einstein, A., Investigations on the Theory of Brownian Movement. In Furth, R., Ed. Dover: 1956.
9. Zwolinski, B. J.; Eyring, H.; Reese, C. E. The Journal of Physical and Colloid Chemistry **1948,** 53, (9), 1426-1453.
10. Larson, J. W.; McMahon, T. B. Inorganic Chemistry **1984,** 23, (14), 2029-2033.

CONCLUSION

A comprehensive assessment has been conducted to investigate the molecular mechanisms responsible for the improved elastic modulus, hardness of PolyButylene Terephthalate Clay Nanocomposites (PBT-PCN) and the Oxygen diffusion in PolyButylene Terephthalate (PBT) polymer using molecular dynamics simulation. Interaction energy between PBT-PCNs constituents and the rate of Oxygen's movement in polymer, diffusion coefficient, conformational changes of polymer were evaluated at temperature 300 K.

The results indicate that the underlying mechanisms of change in crystallinity and improvement in elastic modulus and hardness as proposed altered phase theory are valid. Although the same amount of modified clay is used in the preparation of PBT-PCN and Nylon6-PCN, a change in crystallinity and improvement in elastic modulus and hardness are observed in both systems. It appears that, a polymer with higher crystallinity could require significantly higher attractive and repulsive interaction energies between the polymer and modifier compared to a polymer with lower crystallinity to achieve similar magnitude of percent change in crystallinity and improvement in elastic modulus and hardness of PCN.

The results show that the conformational changes of polymer aid the diffusion of Oxygen gas in PBT polymer. Further, this study reveals that the interaction energy between Oxygen molecule and polymer is the key factor for the Oxygen diffusion in PBT polymer. Based on this study, the rate of Oxygen in polymer is a good way of measuring the Oxygen's movement in a polymer at molecular level.

FUTURE WORK

I used smaller representative molecular models with one Oxygen molecule to understand the molecular mechanisms of diffusion in PBT polymer. However, this work can be continued with larger molecular model based on experimental density. In this work I focused on diffusion mechanisms in pure polymer however further work has to be done on PBT clay nanocomposites to understand the diffusion mechanisms. Further study could provide better comprehensive results on diffusion mechanism in PBT polymer and PBT clay nanocomposites.

APPENDIX

NAMD Input Parameters for MD Simulation

```
# Define Molecular Structure and Initial Coordinates.
Structure               File_name.psf
Coordinates             File_name.pdb

# Define Force-Field Parameters
ParaTypeCharmm          on
Parameters              LauricCharmm
Parameters              MMTCharmm
Parameters              PBTCharmm
Exclude                 scaled1-4
1-4scaling              1.0
Switching               on
Switchdist              24
Cutoff                  30
Pairlistdist            32
Stepspercycle           1

# Define Velocity
Velocities              File_name.vel

# Define Constant Temperature Control
Langevin                on
LangevinTemp            TEMP
LangevinDamping         1

# Define Pressure Control
LangevinPiston          on
LangevinPistonTarget    PRESSURE
LangevinPistonPeriod    200
LangevinPistonDecay     100
LangevinPistonTemp      TEMP

# Define restart files
Dcdfile                 Coor.dcd
Dcdfreq                 2000
VelDCDfile              Vel.dcd
VelDCDfreq              2000
Binaryoutput            no
Restartname             restart
Restartfreq             2000
Restartsave             no
Binaryrestart           no
OutputEnergies          2000

# Define Periodic Boundary conditions
CellBasisVector1        x.   0.   0.
CellBasisVector2        0.  y.   0.
CellBasisVector3        0.   0.   z.
```

```
# Define Constraints
SelectConstraints       on
SelectConstrX           on
SelectConstrY           on
SelectConstrZ           off
Conskfile               File_name.pdb
Conskcol                B
Consref                 File_name.pdb
Consexp                 2
Constraints             on

# Define Simulation
Firsttimestep           0
Numsteps                N
Timestep                0.5
Outputname              File_name
```

Script for Kinetic Energy Calculation

```
set output [open kinnetic.dat w]

set totalframes [molinfo top get numframes]

set sel [atomselect top "resname O2"]

for {set i 0} {$i < $totalframes} {incr i} {

$sel frame $i

$sel frame

foreach m [$sel get mass] v [$sel get {x y z}] {

puts $output [expr 0.5 * $m * [vecdot $v $v] ]

} }

close $output
```

Force Field Parameter Definitions

Bonded Energy $U_{bond} = \sum_{i=1}^{n} K_i^{bond} (r_i - r_{oi})^2$

K_i^{bond} - Spring constant, r_{oi} - Equilibrium distance

Angle Energy $U_{angle} = \sum_{i=1}^{n} K_i^{angle} (\theta_i - \theta_{oi})^2$

K_i^{angle} - Angle constant, θ_{oi} - Equilibrium angle

Dihedral Energy $U_{dihedral} = \sum_{i=1}^{n} K_i^{dihedral}[1 + \cos(n_i\varphi_i - \varphi_{oi})], n_i \neq 0$

$K_i^{dihedral}$ - Multiplicative constant, φ_{oi} - Phase shift angle,

n_i – Non-negative and indicates periodicity

Improper Energy $U_{improper} = \sum_{i=1}^{n} K_i^{improper} (\emptyset_i - \emptyset_{oi})^2$

$K_i^{improper}$ – Multiplicative constant, $\emptyset_{oi}$ - Equilibrium angle

Van der Waals Energy $$\mathbf{U_{vdW}} = \sum_{i} \sum_{j>1} \mathbf{4}\varepsilon_{ij}\left[\left(\frac{\sigma_{ij}}{\mathbf{r_{ij}}}\right)^{12} - \left(\frac{\sigma_{ij}}{\mathbf{r_{ij}}}\right)^{6}\right]$$

ε – Lennard-Jones well depth, σ_{ij} – Lennard-Jones radius

$\varepsilon_{ij} = SQRT(\varepsilon_i * \varepsilon_j)$

Electrostatic Energy $$\mathbf{U_{coulomb}} = \sum_{i} \sum_{j>1} \frac{\mathbf{q_i q_j}}{\mathbf{4}\pi\varepsilon_o \mathbf{r_{ij}}}$$

q_i, q_j – Charges of respective atoms, ε_o-Dielectric constant

r_{ij} – Distance of pair of atoms

X-Ray Diffraction Data

X-Ray diffraction data for Organically Modified Montmorillonite (OMMT) and Poly Butylene Terephthalate Clay Nanocomposites (PBT-PCN) are shown here.

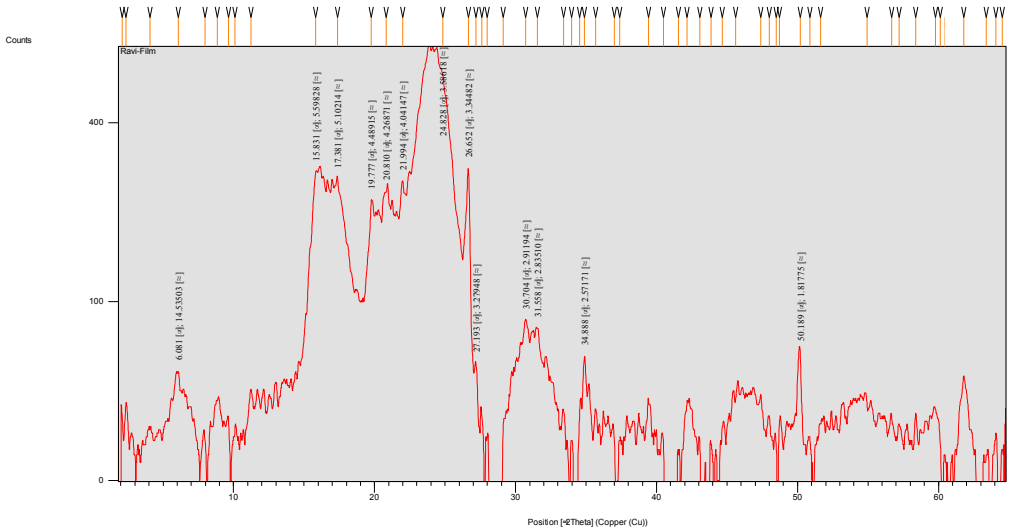

Figure A1. XRD Data of OMMT

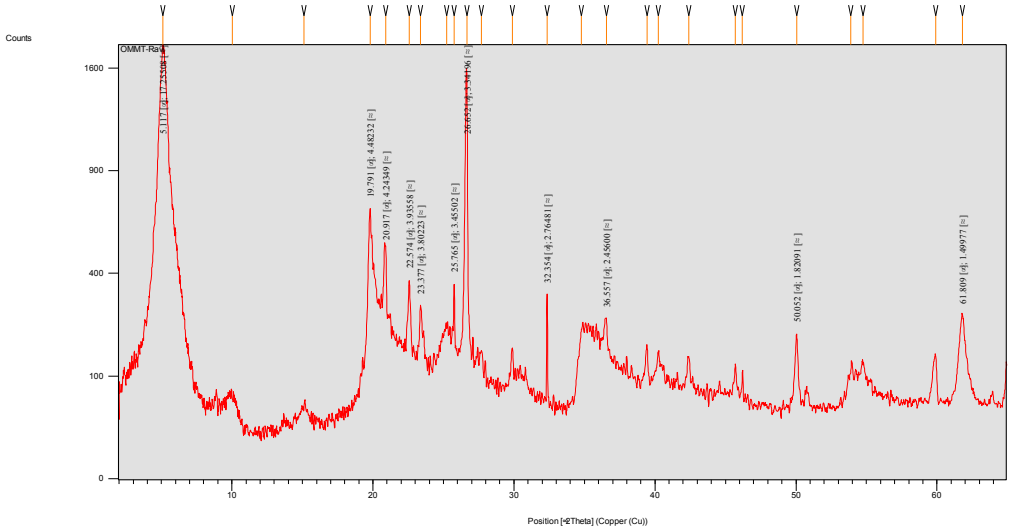

Figure A2. XRD Data of PBT-PCN